JCTC Journal of Chemical Theory and Computation

pubs.acs.org/JCTC Article

Generalizing Double-Hybrid Density Functionals: Impact of Higher-Order Perturbation Terms

Subrata Jana,*,§ Szymon Śmiga,*,§ Lucian A. Constantin,* and Prasanjit Samal*

Cite This: J. Chem. Theory Comput. 2020, 16, 7413−7430 Read Online

ACCESS | Metrics & More | Article Recommendations | Supporting Information

ABSTRACT: Connections between the Görling−Levy (GL) perturbation theory and the parameters of double-hybrid (DH) density functional are established via adiabatic connection formalism. Moreover, we present a more general DH density functional theory, where the higher-order perturbation terms beyond the second-order GL2 one, such as GL3 and GL4, also contribute. It is shown that a class of DH functionals including previously proposed ones can be formed using the present construction. Based on the proposed formalism, we assess the performance of higher-order DH and long-range corrected DH formed on the Perdew−Burke−Ernzerhof (PBE) semilocal functional and second-order GL2 correlation energy. The underlying construction of DH functionals based on the generalized many-body perturbation approaches is physically appealing in terms of the development of the non-local forms using more accurate and sophisticated semilocal functionals.

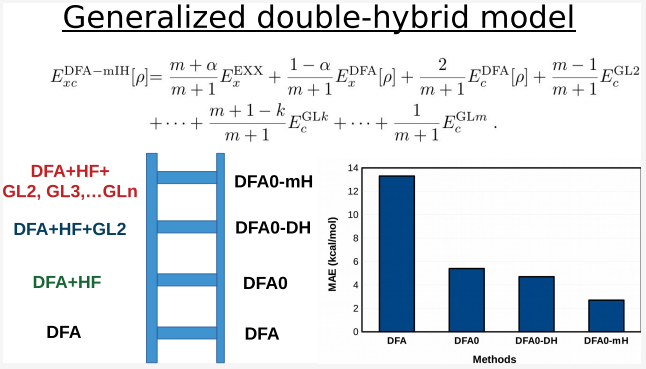

1. INTRODUCTION

Nowadays, density functional theory (DFT)[1,2] becomes a standard framework of performing the electronic structure calculations of atoms, molecules, and solids, being an indispensable tool for quantum chemists and solid-state physicists. Despite its theoretical exactness, in practical calculations, the many-body interactions are included in DFT through density functional approximations (DFA) of the exchange-correlation (XC)[3] energy term. Therefore, the accuracy of the DFT depends on the accuracy of the XC approximations constructed from the exact quantum mechanical constraints satisfaction[4−9] and/or the empirical way.[10−13] The quantum mechanical constraints that have been used to construct the semilocal XC approximations are also equally important for developing higher-order accurate hybrids and double-hybrid (DH) functionals. Within the known exact constraints, we find uniform or non-uniform coordinate transformations,[5,14−16] density gradient expansions,[17−22] high and low-density limit of the correlation energy functionals,[23−25] correct asymptotic behavior of the XC energy density,[26−33] dimensional crossover or the quasi-2D behavior of the XC energy,[34−37] bounds of exchange and XC energies,[38−44] and exact properties of the XC hole.[8,45−47] All of these have been used regularly to construct the different rungs of non-empirical functionals[48] including higher-order accurate wave function methods.

The first three rungs of the XC DFAs,[48] which are recognized as the local density approximation (LDA),[1] generalized gradient approximation (GGA),[49] and meta-generalized gradient approximation (meta-GGA),[50] are constructed using the local or semilocal quantities (i.e., density, the gradient of density, Laplacian of density, and Kohn−Sham (KS) kinetic energy density), being very accurate for the diverse nature of the molecular[51,52] and solid-state properties.[9,53−61] However, there are important limitations in semilocal functionals performance.[62] Several resolutions are adopted to improve the functional performance, such as the inclusion of Hartree−Fock (HF) exchange within the semilocal approximations. Functionals constructed in this way are known as hybrid functionals, being extensively used for the chemical and solid-state properties.[51,63−82] Despite the attempt of constructing the best hybrid density functional, an important dynamic correlation, which is the key of the *ab initio* wave functional theory (WFT), are missing in density functional correlation energy functionals. Inclusion of non-local virtual orbital-dependent terms is shown to overcome many problems of DFAs including the best hybrid density functionals. The resulting functionals developed by mixing a part of second-order Møller−Plesset (MP2)[83] correlation energy expression are known as the DH DFA, which connect the density functional

Received: August 6, 2020
Published: November 18, 2020

https://dx.doi.org/10.1021/acs.jctc.0c00823
J. Chem. Theory Comput. 2020, 16, 7413−7430

world with that of the *ab initio* WFT. Beginning from the Grimme's B2-PLYP[62] DFA, several DH functionals have been proposed (see, e.g., refs 84 and 85 and references therein).

In general, the construction of a DH functional starts from the global hybrid DFA (also known as DFA0) having the form

$$E^{DFA0} = a_x E_x^{EXX} + (1 - a_x)E_x^{DFA} + E_c^{DFA} \tag{1}$$

Also, the range-separated (RS) scheme is applied in the construction of the hybrid density functionals using the RS screening approach of the exchange hole. Such XC functionals are known as the screened hybrids (SH), and they can achieve the correct asymptotic behavior of exchange potentials, important for the barrier heights, charge transfer excitation, and many-electron self-interaction related problems.[86−122] The screening of the exchange energy part is achieved through the decoupling of the electron−electron interaction as

$$\frac{1}{r_{12}} = w_{ee}^{SR,\omega} + w_{ee}^{LR,\omega} = \underbrace{\frac{\mathrm{erfc}(\omega r)}{r_{12}}}_{SR} + \underbrace{\frac{\mathrm{erf}(\omega r)}{r_{12}}}_{LR} \tag{2}$$

where ω is the range-separation parameter. Despite the plethora of considerable successes, there are limitations of both the DFA0 and SH functionals, which have been further improved by mixing the semilocal correlation functional with the non-local, second-order Görling−Levy (GL2), (i.e., MP2-like expression neglecting the single excited term) correlation energy expression

$$E_{xc}^{DH} = a_x E_x^{EXX} + (1 - a_x)E_x^{DFA} + a_c E_c^{GL2} + (1 - a_c)E_c^{DFA} \tag{3}$$

Therefore, the DH DFA is considered as the fifth rung functional where the two parameters $\{a_x, a_c\}$ are fixed either empirically (with respect to the benchmark data) or in the non-empirical way. In particular, there exist two known relations between $\{a_x, a_c\}$ parameters, namely, $a_c = (a_x)^2$ proposed in ref 123, and used by B2-PLYP[62] or DS1DH[123] XC functionals, and the cubic scaling relation[124]

$$a_c = (a_x)^3 \tag{4}$$

which is adopted in the hereto study. The DH functionals achieved their accuracy over a large range of molecular properties beyond the limitations of the DFA0 and SH functionals.[85] In particular, the improvement of many-electron self-interaction problems and non-covalent interactions are noticeable.

The formal construction of the DH was first attempted in ref 125 using the adiabatic connection (AC)-based coupling constant integral formalism, which is the basis of the density functional many-body perturbation theory. Physically, the DH functionals are constructed from the perturbation theory of the XC functionals in the weakly interacting limit where the exchange part is treated by HF, and correlation is approximated by the GL2 expression. The higher-order terms of the perturbation series, i.e., GL3, GL4, etc., can also be used through the perturbation theory to construct the general *m*th-order hybrids (*m*H); however, due to substantial numerical cost of evaluation of these terms, they never have been considered. Nevertheless, in general, a form of the *m*H functional can be proposed, which allows one to include all the higher-order perturbation terms. This is the main motivation of the present study. In this work, we "generalized the double-hybrid density functional" derived from the many-body perturbation theory, which connects the higher-order GL perturbation terms via the adiabatic connection formalism. The novelty of the present method is also attributed via the assessment of the series of double hybrids based on *m*th-order integrand and RS scheme.

In the following, we will present the key equations and features of the prime DH functionals proposed so far. Following this, we will present the theory and results obtained from constructed functionals. We will conclude with future prospects.

2. RUNGS OF DOUBLE-HYBRID DENSITY FUNCTIONS

2.1. Adiabatic Connection View on DH Functionals. The starting point of the construction of DH functionals can be encapsulated through the AC formalism, where the coupling constant integral is used to construct the exact expression of the XC functional as

$$E_{xc}[\rho] = \int_0^1 \mathrm{d}\lambda\, W_{xc,\lambda}[\rho]$$
$$W_{xc,\lambda}[\rho] = \langle \Psi_\lambda[\rho]|\hat{V}_{ee}|\Psi_\lambda[\rho]\rangle - U[\rho] \tag{5}$$

where $\hat{V}_{ee}$, $U[\rho]$, and $\Psi_\lambda[\rho]$ are the Coulomb operator, the Hartree energy, and the anti-symmetric wave function that yields the correct many-electron interacting density $\rho(\mathbf{r})$ and minimizes the expectation value of $\langle \hat{T} + \lambda \hat{V}_{ee}\rangle$, where $\hat{T}$ is the kinetic energy operator and λ is the coupling constant. In the AC formalism, two limiting cases are important for the DH DFA construction, namely, the $\lambda \to 0$ (weak-interaction limit) and $\lambda \to 1$ (full-interaction limit). When $\lambda \to 0$, the GL2[23−25,126] becomes the dominant correction to EXX energy. These two terms are most commonly employed to construct the XC energy integrand in this regime:[24]

$$W_{xc,\lambda\to 0}[\rho] = W_0[\rho] + W_0'[\rho]\lambda \tag{6}$$

where $W_0[\rho] = E_x^{EXX}[\rho]$ and $W_0'[\rho] = 2E_c^{GL2}[\rho]$. We remark, however, that for any small value of λ ($\lambda > 0$), higher-order terms contribute as well. Therefore, one should also consider their inclusion in the $W_{xc,\lambda\to 0}$ integrand. In the full interacting limit, in turn, the $W_{xc,1}[\rho]$ is usually approximated by non-local or semilocal formula.[14,128] Thus, the DH functional connects, by construction, the XC worlds of both the semilocal DFT and WFT approaches.[128] The utilization of the GL2 correlation energy term allows one to include non-local dynamic correlation effects into the XC DFA going beyond the semilocal correlation DFA description.

The AC formalism was applied in the construction of many semi-empirical or non-empirical DH DFAs among which we can recall the DFA0-DH,[129] DFA0-2,[130] DFA-CIDH,[127] or DFA-CIDH[127] DFA-QIDH[131] to be the most successful. In particular, the quadratic integrand DH (QIDH)[131] DFA was constructed considering $W_{xc,\lambda}$ as the quadratic function[132] of λ, i.e., $W_{xc,\lambda}[\rho] = a_1[\rho] + a_2[\rho]\lambda + a_3[\rho]\lambda^2$. In the following, we adopt a general *m*th-order integrand function, which allows one to go beyond the QIDH formalism.

2.2. Beyond the DFA-QIDH Model. Let us consider the XC *m*-hybrid (*m*H) functional defined as

$$E_{xc}^{\mathrm{DFA-mIH}} = \xi_1 E_x^{\mathrm{EXX}} + \xi_2 E_c^{\mathrm{GL2}} + \cdots + \xi_m E_c^{\mathrm{GL}m} + \xi_{m+1} E_x^{\mathrm{DFA}} + \xi_{m+2} E_c^{\mathrm{DFA}} \tag{7}$$

where ξ_k, $k = 1, \ldots, m + 2$ are parameters. The E_x^{DFA} and E_c^{DFA} denote standard semilocal DFAs of exchange and correlation functionals, respectively, whereas the E_x^{EXX} is the HF (or exact) exchange energy:

https://dx.doi.org/10.1021/acs.jctc.0c00823
J. Chem. Theory Comput. 2020, 16, 7413−7430

$$E_x^{EXX} = -\frac{1}{2}\sum_{i,j}\langle ij|ji\rangle \tag{8}$$

where $\langle pq|rs\rangle = \iint \mathrm{d}\underline{x}_1\,\mathrm{d}\underline{x}_2\varphi_p^*(\underline{x}_1)\varphi_q^*(\underline{x}_2)\varphi_r(\underline{x}_1)\varphi_s(\underline{x}_2)/|\underline{r}_2 - \underline{r}_1|$ are the two-electron integrals. The expression for the GL2 correlation energy reads[23]

$$E_c^{\mathrm{GL2}} = -\frac{1}{4}\sum_{abij}\frac{|\langle ij||ab\rangle|^2}{\varepsilon_a + \varepsilon_b - \varepsilon_i - \varepsilon_j} - \sum_{ia}\frac{|\langle i|v_x^{KS} - \hat{v}_x^{HF}|a\rangle|^2}{\varepsilon_a - \varepsilon_i} \tag{9}$$

where $\langle ij||ab\rangle = \langle ij\,|\,ab\rangle - \langle ij\,|\,ba\rangle$ are the antisymmetrized two-electron integrals, and ε_p is the energy of the KS orbital p, whereas v_x^{KS} and $\hat{v}_x^{HF}$ denotes the local, multiplicative KS and the non-local HF exchange potentials, respectively. The higher-order GL energy terms[23,133] are denoted generally as $E_c^{\mathrm{GL}k}$ and the indices i, j, ... and a, b, ... are used to denote occupied and virtual KS orbitals, respectively.

The ξ_i parameters in eq 7 can be, in principle, determined using adiabatic connection formalism, which defines, via eq 5, the exact XC functional. The coupling-constant integrand of eq 5 has the well-known small-λ expansion[24,134]

$$W_{xc,\lambda\to 0}[\rho] = E_x^{\mathrm{EXX}} + \sum_{n=2}^{\infty} n\,E_c^{\mathrm{GL}n}\lambda^{n-1} \tag{10}$$

Hence, truncating the above summation at $n = m$, it reads

$$W_{xc,\lambda\to 0}[\rho] = E_x^{\mathrm{EXX}} + 2E_c^{\mathrm{GL2}}\lambda + \ldots + mE_c^{\mathrm{GL}m}\lambda^{m-1} \tag{11}$$

Now, as in ref 131, we can define W_λ integrand as

$$W_{xc,\lambda} \approx W_\lambda^{m\mathrm{H}}[\rho] = a_1[\rho] + a_2[\rho]\lambda + \cdots + a_m[\rho]\lambda^{m-1} + a_{m+1}[\rho]\lambda^m \tag{12}$$

where a_k ($k = 1, \ldots, m$) are the density or orbital dependent functionals. By comparing eq 11 and eq 12 at $\lambda \to 0$, we get

$$a_1[\rho] = E_x^{\mathrm{EXX}};\ a_i[\rho] = iE_c^{\mathrm{GL}\,i}$$

The $a_{m+1}[\rho]$ can be set from similar reasoning as in ref 131. At the upper limit ($\lambda = 1$), the integrand can be approximated by

$$W_{xc,1}[\rho] \approx \alpha E_x^{\mathrm{EXX}} + (1-\alpha)E_x^{\mathrm{DFA}}[\rho] + 2E_c^{\mathrm{DFA}}[\rho] \tag{13}$$

where the parameter α (together with m) ranging between $[-m,1]$ controls the amount of EXX in eq 7. Comparing eq 12 and eq 13 at $\lambda = 1$, we obtain

$$a_{m+1}[\rho] = (\alpha-1)E_x^{\mathrm{EXX}} + (1-\alpha)E_x^{\mathrm{DFA}}[\rho] + 2E_c^{\mathrm{DFA}}[\rho] - 2E_c^{\mathrm{GL2}} - \cdots - mE_c^{\mathrm{GL}m} \tag{14}$$

Now, employing eq 12 into eq 5 leads, after some algebra, to

$$E_{xc}^{\mathrm{DFA-mIH}}[\rho] = \frac{m+\alpha}{m+1}E_x^{\mathrm{EXX}} + \frac{1-\alpha}{m+1}E_x^{\mathrm{DFA}}[\rho] + \frac{2}{m+1}E_c^{\mathrm{DFA}}[\rho] + \frac{m-1}{m+1}E_c^{\mathrm{GL2}} + \cdots + \frac{m+1-k}{m+1}E_c^{\mathrm{GL}k} + \cdots + \frac{1}{m+1}E_c^{\mathrm{GL}m} \tag{15}$$

Direct comparison with eq 7 allows to connect (in the quantize manner) the ξ_i parameters with orders of the GL perturbation theory as

$$\xi_1 = \frac{m+\alpha}{m+1};\ \xi_2 = \frac{m-1}{m+1};\ \xi_k = \frac{m+1-k}{m+1}$$

$$\xi_{m+1} = \frac{1-\alpha}{m+1};\ \xi_{m+2} = \frac{2}{m+1}$$

Note that, when $m \to 1$, we get

$$E_{xc}[\rho] = \frac{1+\alpha}{2}E_x^{\mathrm{EXX}} + \frac{1-\alpha}{2}E_x^{\mathrm{DFA}}[\rho] + E_c^{\mathrm{DFA}}[\rho]$$

On the other hand, when $m \to \infty$, eq 15 recovers

$$E_{xc}[\rho] = E_x^{\mathrm{EXX}} + \sum_{n=2}^{\infty}E_c^{\mathrm{GL}n} \tag{16}$$

which, in general, exhibits a diverging behavior.[135,136] For an arbitrary (but small) value of m, the kth GL terms in eq 15 are always scaled by the coefficient $\xi_k << 1$. Thus, the diverging behavior of DFA-mIH DFA should be avoided.

2.3. Generalized *m*th Hybrid with Range-Separation Model. Having eq 15, the obvious viable next step is to extend it to the domain of the range-separated DH (RSDH) framework. The background of the perturbative RS functionals, it was initially adopted by Ángyán *et al.*[137] Later, the RSDH was adopted by Chai *et al.*[138] in ωB97X family of functionals (ωB97X-2) and by Brémond *et al.*[139,140] in QIDH-based functionals (RSX-QIDH). Both the ωB97X-2 and RSX-QIDH showed an improvement over the base ωB97X and QIDH functionals. Particularly, a significant improvement has been observed for the problems related to the self-interaction corrections, barrier heights, and ionization potential, which are important and viable for RSDH.

In this respect, we extend the generalized formalism presented in Section 2.2 to the RS scheme. By using $W_{xc,1}[\rho] \approx E_x^{EXX,\,LR}(\omega) + E_x^{DFA,\,SR}(\omega) + 2E_c^{DFA}$, we obtain the following expression:

$$E_{xc}^{\mathrm{LRC}-\omega\mathrm{DFA}-\mathrm{mH}}[\rho] = \frac{m}{m+1}E_x^{\mathrm{EXX}} + \frac{1}{m+1}[E_x^{DFA,SR}(\omega) + E_x^{EXX,LR}(\omega)] + \frac{2}{m+1}E_c^{\mathrm{DFA}}[\rho] + \frac{m-1}{m+1}E_c^{\mathrm{GL2}} + \cdots + \frac{m+1-k}{m+1}E_c^{\mathrm{GL}k} + \cdots + \frac{1}{m+1}E_c^{\mathrm{GL}m} \tag{17}$$

Similarly to the DFA-mIH family of functionals, the LRC-ωDFA-mH functionals also depend on the choice of two parameters, namely, m and ω. This is done by disregarding the dependence on the α parameter in eq 17. Note that, in this case, the present RS functional form is closely related to the LRC-ωPBEh decomposition proposed by Rohrdanz *et al.*,[94] which reduces to the standard PBEh hybrid for a certain choice of the two parameters, namely, mixing (a_x) and range-separated (ω) parameters.

We underline, however, that by choosing $W_{xc,1}[\rho] \approx \alpha E_x^{EXX} + (1-\alpha)[E_x^{DFA,\,SR}(\omega) + E_x^{EXX,\,LR}(\omega)] + 2E_c^{DFA}$, we can define also the family of RSX-mIH functionals, where for $m = 2$ we recover the RSX-QIDH[139,140] DFA.

2.4. Choice of Functionals and α and ω Parameters. Based on the generalized consideration presented in Sections 2.2 and 2.3, we consider two forms of the functionals to assess their

https://dx.doi.org/10.1021/acs.jctc.0c00823
J. Chem. Theory Comput. 2020, 16, 7413−7430

performance for the quantum chemistry test sets. However, due to the substantial computational cost of the inclusion of higher-order GL terms, we restrict our assessment to DFAs whose form include only the second-order GL2 term (in eqs 15 and 17) and m = 2,3,4. The impact of higher-order terms is discussed in Section 3.1.

In eq 15, for the semilocal part of XC approximation, we consider the PBE and thus we denote this family of functionals as PBE-mIDH (m, α) as it is based on the mth-order integrand limited to second order and the m and α parameters. In the second case, we investigate LRC-ωDFA-mH functionals defined via eq 17) where, as the SR part of DFA, we have chosen the ωPBE[92] functional and therefore the functional family is denoted as LRC-ωPBE-DH (m, ω) as it is based on the m and empirically fitted ω.

In order to make the PBE-mIDH and LRC-ωPBE-DH methods feasible, we need to set the values of α and ω parameters, respectively. In the case of α, we can directly utilize the cubic scaling relation ($\xi_2 = \xi_1^3$) from ref 124 usually adopted in the construction of novel DH DFAs. This allows one to express α as a function of m:

$$\alpha(m) = (m^3 + m^2 - m - 1)^{1/3} - m \quad (18)$$

Thus, the PBE-mIDH family of functionals can be considered as "non-empirical" in this sense. The present PBE-mIDH model not only correctly recovers the PBE-QIDH[131] for m = 2, but also it recovers the PBE0-2[130] functional for m = 3. This allows one to view the construction of the PBE0-2 functional from an entirely new physical point of view. As m = 2 and m = 3 are the two previously proposed functionals, here, we additionally assess the functional performance for m = 4.

In the case of the LRC-ωPBE-DH (m, ω) family of functionals, we cannot establish a direct relation between m and ω. Thus, in order to determine the ω screened parameter, several schemes can be utilized, such as empirical fitting,[89,92,95,99,119,141] optimal tuning,[142] or imposing an additional constraint to the XC functional.[139,143]

In this study, in order to be consistent with the LRC-ωPBEh functional, we have tuned ω considering the mean absolute error (MAE) of the small representative test sets AE6 and BH6.[144] The AE6 is the atomization energies of six molecules simulating the error statistics of the full G2/148 molecular test set. Meanwhile, the BH6 is the hydrogen transfer barrier heights of six small molecules. In the optimization procedure, we have used the AE6 and BH6 geometries from Lynch and Truhlar,[144] and for the reference values, we consider the non-relativistic coupled-cluster singles-doubles with perturbative triples (CCSD(T)[145] values [FC-CCSD(T)/cc-pVQZ-F12] of ref 146.

In Figure 1, we report the MAE of AE6 and BH6 for few values of m. We observe that, for m = 2, the minimum of the MAE becomes at ω = 0.2 bohr^{-1}. This choice of {m = 2, ω = 0.2} is certainly a good choice for BH6 also, where the MAE is obtained to be about 1 kcal/mol smaller than the LC-ωPBE and LRC-ωPBEh. Interestingly, in ref 94, the choice of ω is also 0.2 bohr^{-1}, which is certainly matching with our present LRC-ωPBE-DH functional.

In Table 1, we present the parameters {m, α} and {m, ω} of the studied functionals. Note that, for LRC-ωPBE-DH (m = 3, ω), we chose ω = 0.2 bohr^{-1}, which gives a balanced description of both AE6 and BH6, while for LRC-ωPBE-DH (m = 4, ω), we chose ω = 0.5 bohr^{-1}, considering solely the optimization of the AE6 test set.

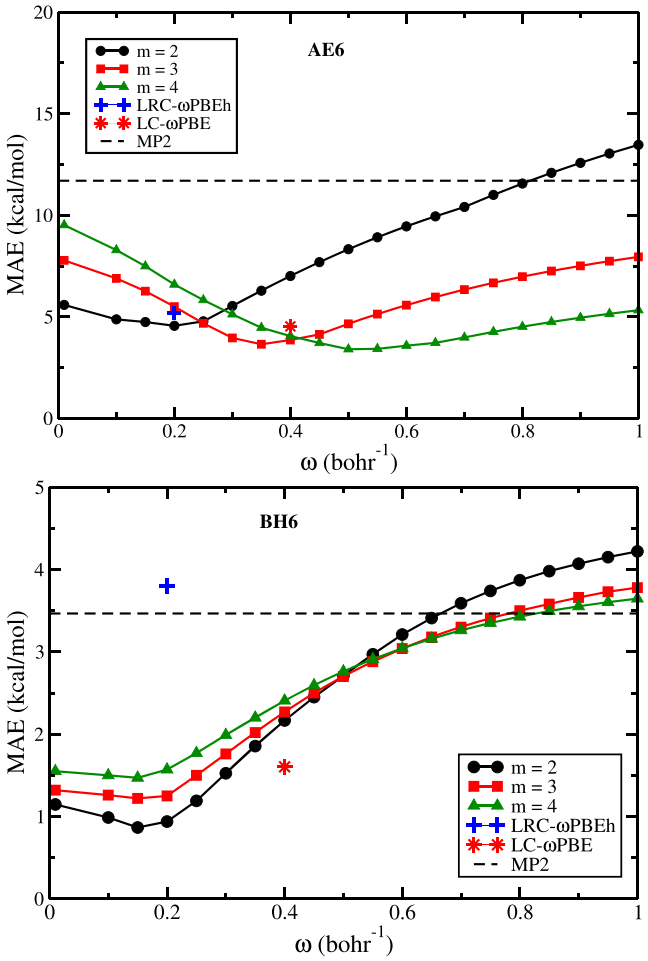

Figure 1. MAE (in kcal/mol) of AE6 and BH6 test sets for different values of m and ω.

Table 1. Choice of Different Sets of {m, α} and {m, ω} as Used in the Calculations[a]

PBE-mIDH (m, α)		LRC-ωPBE-DH (m, ω)			
m	α[1]		m	ω	MAE (kcal/mol)
2	0.080	AE6/BH6	2	0.2	5.5/1.08
3	0.175	AE6/BH6	3	0.2	5.3/1.38[2]
4	0.217	AE6/BH6	4	0.5	4.2/2.84

[a]The ω values are in bohr^{-1} unit. [1]Obtained via Eq. (18). [2]Minimum of AE6 is obtained at ω = 0.35 bohr^{-1} (3.6 kcal/mol) but choice of ω = 0.20 bohr^{-1} is the most preferable for both the AE6 and BH6.

3. RESULTS

In this section, we discuss the general trends found in the performance of both families of functionals. The details about the computational setup can be found in Section 5.

3.1. Impact of the Higher-Order Terms on the Functional Performance. In Table 2, we report the MAE and mean absolute relative error (MARE) obtained for several *ab initio* WFT approaches together with the results obtained for both families of DH DFAs. The errors have been calculated with respect to CCSD(T) data obtained using the same computational setup. Additionally, to investigate the impact of higher-order terms (HOT) on the quality of predictions, we report the triple-hybrid (TH) (PBE-TH, LRC-ωPBE-TH) and quadruple-hybrid (QH) (PBE-QH, LRC-ωPBE-QH) results. To this end,

https://dx.doi.org/10.1021/acs.jctc.0c00823
J. Chem. Theory Comput. 2020, 16, 7413−7430

Table 2. Error Statistic on Total Energies, Atomization Energies of AE6, and Binding Energies for Several *Ab Initio* Wave-Function Theory and Density Functional Theory Methods[a]

					PBE-mIDH					LRC-ωPBE-DH				
	CCSD	MP2	MP3	MP4	$m = 2$	$m = 3$	$m = 4$	PBE-TH	PBE-QH	$m = 2$	$m = 3$	$m = 4$	LRC-TH	LRC-QH
Total energies (TE)[1]														
MAE [mHa]	8.93	16.81	11.82	2.42	5.57	6.14	7.11	5.08	3.11	5.25	5.86	6.84	4.81	4.92
MARE [%]	0.01	0.09	0.03	0.01	0.04	0.04	0.05	0.03	0.02	0.03	0.04	0.03	0.03	0.01
AE6[1]														
MAE[3]	10.3	12.4	6.7	5.9	4.0	4.7	6.2	3.8	2.7	3.5	4.5	2.3	3.4	4.3
MARE [%]	3.01	3.58	2.36	1.59	1.34	1.23	1.68	1.08	0.61	1.10	1.08	0.71	1.03	1.63
Non-covalent interactions (NCI)[2]														
MAE[3]	0.17	0.13	0.05	0.04	0.08	0.09	0.09	0.07	0.06	0.09	0.06	0.05	0.07	0.07
MARE [%]	16.27	20.76	10.17	3.49	20.21	19.90	19.39	19.16	15.22	41.40	32.06	34.64	32.46	33.27

[a]The full results can be found in ref 147. The LRC-TH and LRC-QH denotes LRC-ωPBE-TH and LRC-ωPBE-QH, respectively. [1]Calculation performed in cc-pVQZ basis set, all electrons are correlated. [2]Calculation performed in aug-cc-pVQZ basis set, all electrons are correlated. [3]In kcal/mol.

the energies have been calculated via eqs 15 and 17 taking into account all terms up to mth order, on top of GKS orbitals obtained for $m = 3$ and $m = 4$ for TH and QH, respectively. As aforementioned, in order to evaluate the higher-order GLk energy contributions (GL3, GL4), we utilize the MP-like formulas (MP3 and MP4) (evaluated on the same GKS reference state), which give the dominant energy contribution. This is mostly dictated by the lack of quantum chemistry codes that are capable to calculate full higher-order GLk terms (see Section 5 for more details).

In the case of total energies (TE), both MAE and MARE indicate that all DH DFAs give the results at least twice better than MP2 total energies, which yield a MAE of 16.81 mHa (MARE = 0.09%). The addition of HOT leads to further improvement. In the case of TH, the inclusion of the GL3 term leads to a decrease in MAE/MARE of about 1 mHa/0.01%, whereas for QH, the decrease is slightly larger (2 ÷ 3 mHa/0.02 ÷ 0.03%) in comparison to their $m = 3$ and $m = 4$ DFA counterparts. Moreover, one can note that TH and QH DFAs give results that lie between MP3 and MP4 predictions. This indicates that the inclusion of HOT might lead to quite substantial improvement of the results than the standard DH expressions.[148]

In the case of the AE6 atomization energies, we see that all DH DFAs outperform all reported *ab initio* WFT methods. Here, the worst performance is observed for the MP2 method (MAE = 12.4 kcal/mol, MARE = 3.58%) and surprisingly also for the CCSD method (MAE = 10.3 kcal/mol, MARE = 3.01%). In the case of the PBE-mIDH family of DFA, we see the worsening, and for LRC-ωPBE-DH, the improvement of the predictions along with an increase in m. For the latter species, this can be easily linked with the optimization of the ω parameter, which was performed with respect to the AE6 set. One can note that inclusion of HOT in both families of DFAs lead, in general, to improvement in the prediction. The PBE-TH and PBE-QH functionals improve upon their DH counterparts, giving here a MAE of 3.8 kcal/mol (MARE = 1.08%) and a MAE of 2.7 kcal/mol (MARE = 0.61%), respectively. In the case of LRC-ωPBE-TH, we observe a similar trend. The only exception is seen in the case of LRC-ωPBE-DH ($m = 4$) and LRC-ωPBE-QH DFAs where the latter exhibits almost twice worse performance with respect to its DH variant. This can be most probably related to the ω value, which is not optimal for the LRC-ωPBE-QH energy expression.

In order to check how these trends change for AE6 with basis set size, in Fig. S5 of Ref 147., we report the MARE calculated with respect to CCSD(T) data obtained using the cc-pVXZ[149] basis set family (where X = D, T, Q). As one can note, for most of DFAs we observe, a drastic improvement between DZ and TZ results. The differences between TZ and QZ results are several times smaller. One exception can only be noted for LRC-ωPBE-DH ($m = 4$) and LRC-ωPBE-QH functionals. Here, the DZ results are quite similar to TZ and QZ counterparts. As previously noted, this behavior can be related to the ω value, which was optimized solely with respect to the AE6 data set. Nevertheless, we conclude that, for the DZ basis set, all DFAs give the worst performance, whereas TZ and QZ results do not differ significantly from each other.

Finally, we have tested all DFAs with respect to a small set of NCI systems.[150] Similar to AE6 data, the worst performance among WFT approaches is given by CCSD (MAE = 0.17 kcal/mol, MARE = 16.27%) and MP2 (MAE = 0.13 kcal/mol, MARE = 20.76%) methods. The MP4, in turn, gives the best predictions here, yielding a MAE of 0.04 kcal/mol (MARE = 3.49%). All PBE-mIDH functionals show almost the same performance with MAEs in the range of 0.08−0.09 kcal/mol (MARE between 19.39% and 20.21%). The addition of HOT terms, also here, leads to an improvement mostly visible for PBE-QH DFA, which gives a MAE of 0.06 kcal/mol (MARE = 15.22%). In the case of the LRC-ωPBE-DH family of functionals, the inspection of MAEs shows almost identical performance (MAE between 0.5 and 0.09 kcal/mol) for all DFAs. However, MAREs exhibit a substantial increase in error (almost twice), which is caused by the very bad performance of LRC-ωPBE-DH (large MAE) for weakly interacting systems (see Tab. S2 in ref 147). In ref 147, we also report MAE and MARE without considering WI systems. One can immediately note the substantial decrease in MARE values mostly visible for the LRC-ωPBE-DH family of functionals. This indicates that WI binding energies can be considered as very sensitive tools for testing the quality of quantum chemistry methods.

To conclude, the inclusion of HOT leads in general to the improvement of the result. However, the substantial cost of MP3-like and MP4-like correlation contribution makes it almost impossible to apply, especially for large molecular systems.

3.2. Performance without Considering HOT. *3.2.1. Molecular Properties.* To assess the PBE-mIDH and LRC-ωPBE-DH families ($m = 2,3,4$) of functionals, we report in Table 3 the MAEs for several standard benchmark tests. For comparison, we

https://dx.doi.org/10.1021/acs.jctc.0c00823
J. Chem. Theory Comput. 2020, 16, 7413−7430

Table 3. Mean Absolute Errors (MAE) (in kcal/mol) for the Benchmark Tests Obtained Using Various Double-Hybrid Functionals[a]

	MP2	PBE0-DH	PBE-QIDH (m = 2)	PBE0-2 (m = 3)	PBE-mIDH (m = 4)	LRC-ωPBE-DH (m = 2)	LRC-ωPBE-DH (m = 3)	LRC-ωPBE-DH (m = 4)	PBE0	LC-ωPBE (ω = 0.40)[1]	RSX-QIDH
Main group thermochemistry (MGT)											
AE6	11.6	5.8	5.3	5.3	6.0	5.5	5.3	**4.2**	5.4	5.0	7.0
G2/148	10.7	5.7	5.4	5.6	6.2	5.3	5.4	4.9	4.5	**4.4**	7.8
G21EA	4.02	3.39	3.03	2.75	2.75	3.30	**2.72**	3.52	2.91	2.98	3.39
G21IP	3.37	3.31	2.64	2.23	**2.11**	2.85	2.21	2.62	3.78	4.78	3.12
PA26	1.52	2.55	2.04	1.60	**1.38**	2.20	1.60	1.80	2.52	2.60	1.80
BH76RC	2.50	**1.44**	1.52	1.68	1.82	**1.51**	1.69	1.78	1.59	3.62	2.12
SIE4×4	1.62	7.36	3.33	1.68	**0.99**	2.67	2.00	1.88	14.12	9.42	1.91
TMAE	5.04	4.22	3.32	2.97	3.13	3.33	2.98	**2.95**	4.97	4.68	3.87
Barrier heights (BH)											
BH6	3.54	1.85	**0.88**	1.39	1.82	**1.08**	1.38	2.84	4.59	1.39	1.42
HTBH38	3.61	1.53	**0.95**	1.50	1.89	1.11	1.48	2.97	4.21	1.20	1.28
NHTBH38	5.49	**1.70**	1.78	2.55	3.04	2.20	2.63	4.82	3.76	2.22	2.57
TMAE	4.21	1.69	**1.20**	1.81	2.25	**1.46**	1.83	3.54	4.18	1.60	1.75
Non-covalent interactions (NCI)											
HB6	0.24	0.31	0.29	0.31	0.32	0.26	**0.24**	0.25	0.32	0.71	0.91
DI6	0.57	0.30	0.24	0.25	0.32	0.28	0.22	**0.20**	0.36	0.81	0.30
CT7	0.56	0.44	0.40	0.42	0.44	0.33	0.31	**0.27**	0.84	1.12	0.57
PPS5	1.48	1.12	0.36	0.34	0.55	0.46	**0.26**	0.63	1.89	1.96	0.27
WI7	**0.04**	0.16	0.14	0.11	0.10	0.18	0.14	0.13	0.16	0.28	0.15
S22	1.39	1.60	0.74	**0.26**	0.37	0.92	0.34	0.28	2.37	2.75	0.71
TMAE	0.71	0.66	0.36	0.28	0.35	0.41	**0.25**	0.29	0.99	1.27	0.49
Overall											
TMAE	3.32	2.19	**1.63**	1.69	1.91	1.73	1.69	2.26	3.38	2.52	2.04

[a]The least MAE in each category is marked in bold. The total MAE (TMAE) is also mentioned at the bottom of each category. [1]ω = 0.40 bohr^{-1} as suggested in ref. 141

https://dx.doi.org/10.1021/acs.jctc.0c00823
J. Chem. Theory Comput. 2020, 16, 7413−7430

also supplied the results obtained from PBE0-DH, PBE0, LC-ωPBE, and RSX-QIDH methods. Note that, except LC-ωPBE and PBE0, all other functionals belong to DH DFA species.

One can immediately note that all DH functionals outperform the global hybrid PBE0 and RS hybrid LC-ωPBE in all cases. This indicates that the addition of the scaled MP2 term leads, in general, to the improvement of the results with respect to its global or RS hybrid predecessor.

The overall performance of all DH DFAs is quite similar. The total MAEs (TMAEs) can be found in the range of 1.63−2.26 kcal/mol. The best TMAE of 1.63 kcal/mol is given by PBE-QIDH (m = 2), which is closely followed by PBE0-2 (m = 3, TMAE = 1.69 kcal/mol) and LRC-ωPBE-DH (m = 3, TMAE = 1.69 kcal/mol) functionals. Slightly worse results are provided by LRC-ωPBE-DH (m = 2, TMAE = 1.73 kcal/mol) and PBE-mIDH (m = 4), which gives a TMAE of 2.26 kcal/mol. One can also identify general trends in the results depicted in Figure 2

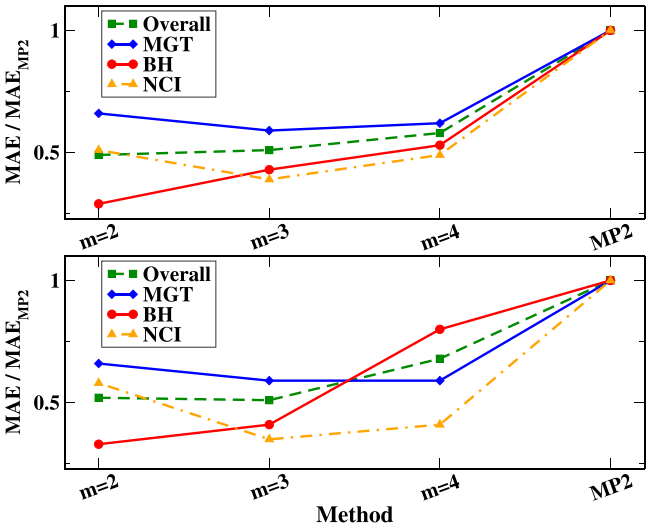

Figure 2. Overall and detailed (MGT, BH, and NCI subsets) trends in the results obtained for (top) PBE-mIDH and (bottom) LRC-ωPBE-DH families of functionals.

where we report the ratio of MAE (for m = 2,3,4) with respect to the MAE of the MP2 method (MAE_{MP2}), which represents the $m = \infty$ case for both families of functionals. In the case of PBE-mIDH DFAs (top of Figure 2), increasing the amount of HF and MP2 terms leads, in general, to the worsening of the predictions. However, all functionals perform much better than the MP2 method. The change in overall performance between the m = 2 and m = 3 cases is very small. Nevertheless, an inspection of subset performance reveals some interesting trends. For the BH subset, we observe evident worsening of the results with m, whereas for MGT, the worse performance between DH cases is observed for m = 2. Here, along with m, we note worsening (AE6, G2/148, BH76RC) and improvement (G21EA, G21IP, PA26, SIE4×4) of the predictions. Almost the same is valid for the NCI subset, where the best performance is obtained for the m = 3 variant. This behavior is, however, dominated by the PPS5 and S22 results, which for m = 3 give the least MAE. For other NCI subsets, we observe the increasing (HB6, DI6, CT7) or decreasing (WI7) trend in MAE with an increase in m. Similar trends can be observed for the LRC-ωPBE-DH family of functionals (bottom of Figure 2). The amount of HF and MP2 terms governs the general behavior of DFAs. With increasing m, we observe the improvement of the results for MGT and worsening for BH. In the case of NCI, likewise for the PBE-mIDH family of functionals, with increasing m, we observe an improvement in the description of most types of interactions especially visible for S22 subsets. This is in more detail shown in Table 4, where we report separately the MAEs for different subsets of complexes in the S22 test set. The PBE0-2 (m = 3) performs significantly better for vdW and mixed complexes. Meanwhile, LRC-ωPBE-DH (m = 3) is better for H-bonded complexes. This behavior can be probably justified by the fact that, for larger values of m, the SCF orbitals (optimized in the presence of 100% LR HF exchange term) give a better starting point (by reducing self-interaction error) for the description of long-range dispersion interaction included in the MP2 term. This is clearly seen in the case of the LRC-ωPBE-DH (m = 4) functional, which gives good performance for NCI and MGT benchmark sets, yielding here MAEs of 0.29 and 2.95 kcal/mol, respectively.

Looking at the MP2 results (representing the $m = \infty$ case), one can note that it gives the worst MAE for all benchmark sets (MAE = 3.32 kcal/mol). This finding suggest that the relative good performance of DH functionals rely on the mutual error cancellation effect between non-local HF and MP2 and semilocal DFA counterparts[148] (see also Section 3.1).

As to the RSX-QIDH DFA performance, it gives an almost identical behavior as PBE0-DH. They both perform similarly for BH and NCI benchmark sets. One can note that RSX-QIDH gives much better performance only for MGT where it yields a MAE of 3.87 kcal/mol, what is still larger in error than the results given by LRC-ωPBE-DH (m = 2) DFA. It is also worth mentioning that RSX-QIDH improves over PBE-QIDH only for PA26 and SIE4×4 subsets while its performance remains unsatisfactory for all other benchmark sets. This is also the case for vertical ionization potentials (VIP) calculated as an energy difference (see G21IP results and discussion in Section 3.2.4).

What is worth noting that, for the SIE4×4 test set, LRC-ωPBE-DH (m = 4) gives twice worse results (MAE = 1.88 kcal/mol) than the PBE-mIDH (m = 4) counterpart, which gives here MAE = 0.99 kcal/mol. The identical trend is observed for the m = 3 case, whereas for m = 2, we observe the improvement of the results (PBE-QIDH gives a MAE of 3.33 kcal/mol, whereas LRC-ωPBE-DH gives MAE = 2.67 kcal/mol). This behavior can be justified from the percentage of the (LR-)HF mixing with the semilocal DFAs. Note that the SIE4×4 test set consists of H_2^+, He^+, NH_3^+, and H_2O^+ molecules (at several points along a dissociation curve of each of the complexes) important to study the problem related to (many-electron) self-interacting error

Table 4. Mean Absolute Errors (in kcal/mol) of the Subsets (H-Bond, Dispersion, and Mixed Complexes) of the S22 Test

interactions	MP2	PBE0-DH	PBE-QIDH (m = 2)	PBE0-2 (m = 3)	PBE-mIDH (m = 4)	LRC-ωPBE-DH (m = 2)	LRC-ωPBE-DH (m = 3)	LRC-ωPBE-DH (m = 4)	RSX-QIDH
H-bond	0.44	0.54	0.35	0.38	0.42	0.41	**0.28**	0.35	1.18
vdW	2.49	2.99	1.38	**0.28**	0.43	1.66	0.53	0.33	0.74
mixed	1.05	1.08	0.41	**0.12**	0.25	0.57	0.19	0.18	0.23

https://dx.doi.org/10.1021/acs.jctc.0c00823
J. Chem. Theory Comput. 2020, 16, 7413−7430

((ME)SIE).[151−156] The PBE-mIDH family of functionals mixes HF more upon increasing m values and shows less many-electron self-interaction error. In other sense, more HF mixing with DFA eliminates the delocalization error of DFAs as the HF is more localized. Similar trends are observed for the LRC-ωPBE-DH family of functionals. For MP2, we observe overestimation in the case of H_2O^+, indicating that the error cancellation from DFAs and HF mixing is important for H_2O^+. However, the error of RSX-QIDH is slightly larger than that of LRC-ωPBE-DH (m = 4).

Here, a bit of analysis of the screened functionals in terms of the dependence on both m and ω is required from the standpoint of performances of the LRC-ωPBE-DH family of functionals. This can be somehow explained by analyzing Figure 1 and Table 3. From Figure 1, one can note that, with increasing ω values, we observe the significant worsening of the results especially visible for the BH6 set. The full MP2 method results can be recovered by going with $m \to \infty$ and $\omega \to \infty$. From eq 17, in turn, we see that, when $\omega \to 0$, we should recover most PBE-mIDH family of functional results. From Table 3, it is also noticed that the main differences in the performance of SIE4 × 4 comes from the different mixtures of the HF percentage, where LRC-ωPBE-DH (m = 4) gives the least error within the LRC-ωPBE-DH (m) family of functionals. Overall, LRC-ωPBE-DH (m = 3) performs better within this family of methods, which may come from the balanced treatment of the HF exchange and MP2 correlation with semilocal parts of the functional.

3.2.2. Dissociation Curves of H_2^+, He_2^+, and ArKr$^+$. In Figure 3, we show the dissociation curves of three representative test cases where the errors of functionals are dominated by the many-electron self-interaction problem.

The dissociation of the H_2^+ molecule (upper panel) can be considered as a paradigm in quantum chemistry,[157] describing the delocalization errors of XC functionals. This system is composed by one electron, such that E_c = 0, and the exchange energy compensates the Hartree energy.[158] We observe that PBE and PBE0 fail badly, showing huge delocalization errors at large internuclear distances, due to their XC hole densities.[159] The LC-ωPBE improves over PBE and PBE0 but is still considerably worse than PBE-mIDH (m = 4) and especially LRC-ωPBE-DH (m = 4), which is very close to the exact HF curve. We recall that the u-metaGGA exchange functional, which uses as an additional ingredient the Hartree potential, is exact for this system.[158]

Next, we consider the dissociation curves of rare gas cation dimers,[156] the He_2^+ (middle panel), and the asymmetric ArKr$^+$ molecule (lower panel). In both cases, the PBE and PBE0 are showing delocalization errors. On the other hand, PBE-mIDH (m = 4) and LRC-ωPBE-DH (m = 4) are very accurate, being close to the CCSD(T) reference, at any internuclear distance R. Moreover, for the He_2^+ molecule, the HF and even MP2 show localization errors at large R,[157] while LRC-ωPBE-DH (m = 4) is almost exact. We also note that for H_2^+ and He_2^+ molecules LRC-ωPBE-DH (m = 4) improve significantly over the RSX-QIDH functional (reported in Fig. 1 in ref 140).

These results, corroborating with the ones for the SIE4×4 test shown in Table 3, prove that PBE-mIDH (m = 4) and LRC-ωPBE-DH (m = 4) are good candidates for real and difficult applications of quantum chemistry.

3.2.3. Correlation Potentials and Densities. In Figure 4 and Figure 5, we report the correlation potentials of PBE-mIDH and LRC-ωPBE-DH families of functionals, respectively, for two representative cases, namely, Ne atom and CO molecule.

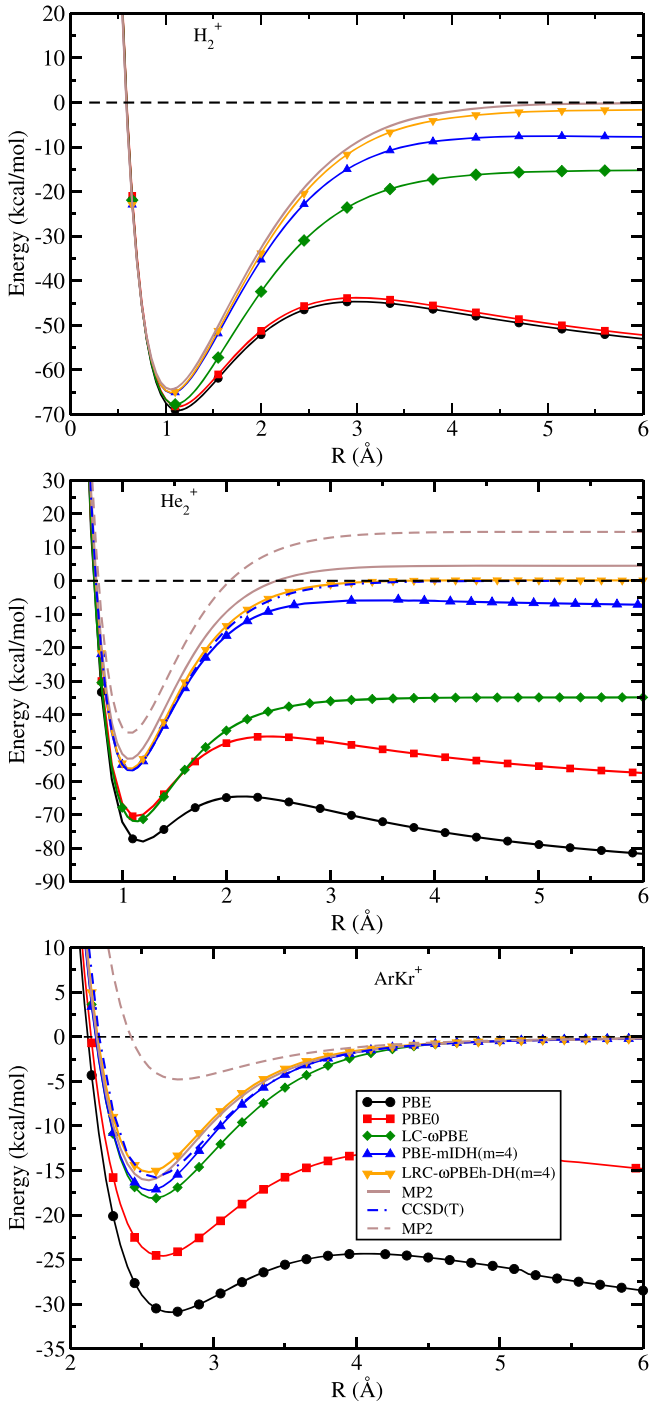

Figure 3. Dissociation curves of H_2^+ (upper panel), He_2^+ (middle panel), and ArKr$^+$ (lower panel).

One can note that all DH DFAs reproduce quite reasonable the physical features of reference correlation potential obtained from the self-consistent *ab initio* OEP2-sc[148,165] method and the one reconstructed from CCSD(T) relaxed density (KS[CCSD(T)]) via a WY inverse approach.[164]

The differences mostly occur in the core (due to Laplacian of the density[166,167] term in GGA potentials[168]) and asymptotic regions (due to the differences in the asymptotic behavior between OEPx ($-1/r$) and semilocal DFAs[169]). The oscillation in both regions are significantly diminished for LRC-ωPBE-DH potentials, which are quite similar to those obtained with OEP2-

https://dx.doi.org/10.1021/acs.jctc.0c00823
J. Chem. Theory Comput. 2020, 16, 7413−7430

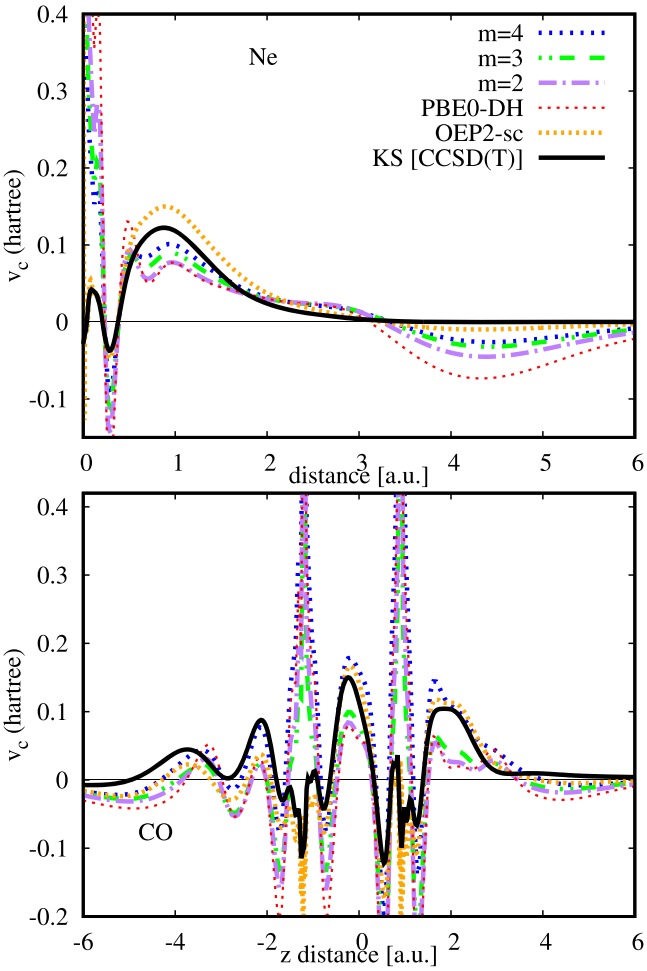

Figure 4. Correlation potentials of the Ne (uncontracted ROOS-ATZP[160]) atom and CO molecule (uncontracted cc-pVTZ,[149] R_0 = 1.128Å) for various PBE-mIDH methods (m = 2 (PBE-QIDX), m = 3 (PBE0-2), and m = 4) obtained using a one-step scheme via the optimized effective potential (OEP) method from refs 161−163. The reference KS[CCSD(T)] has been obtained using a method from ref 164 using the same computational setup.

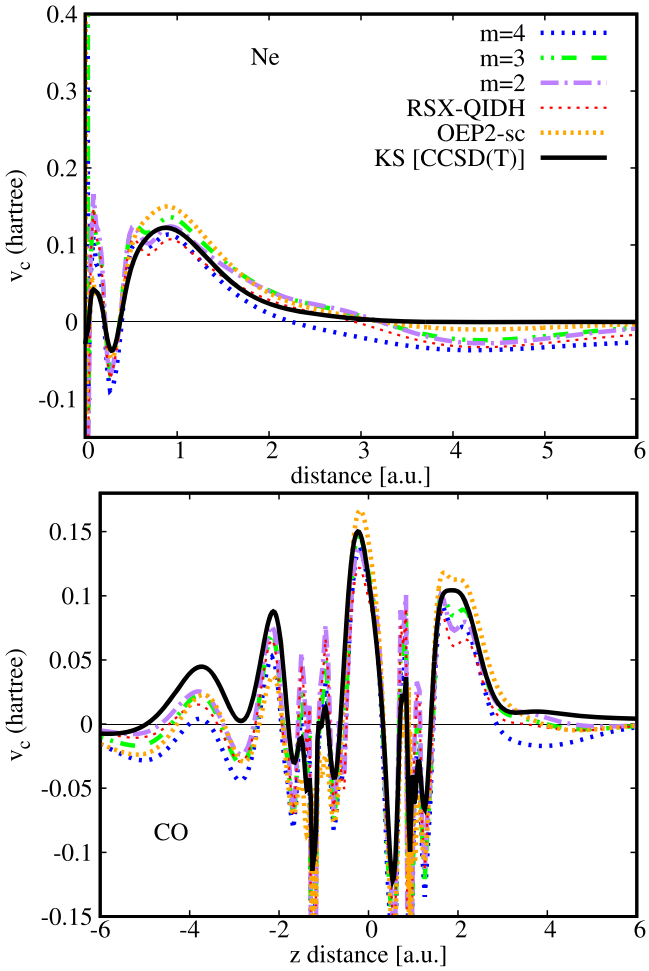

Figure 5. Similar as in Figure 4, but for the LRC-ωPBE-DH (m = 2,3,4) family of functionals.

SOS[170] or interaction-strength interpolation methods.[171] In the asymptotic region, this is due to the incorporation of a proper long-range asymptotic ($-1/r$) behavior in the XC potential via LR part of the EXX term. This feature has a visible impact on the quality of VIP potentials obtained directly from the HOMO energy (see Section 3.2.4 for more details). In the core region, in turn, the LR EXX potential introduces small but non-vanishing contribution,[101,163] which, combined with mutual error cancellation between exchange and correlation part of DFA, leads to a reduction of nonphysical oscillations.

As to the accuracy of methods, one can note that with increasing m the DFAs seem to better reproduce the reference CCSD(T) correlation potentials. Note also that both the PBE0-DH and RSX-QIDH v_c are quite similar in shape with the m = 2 variants differing only in the asymptotic region. For the $m = \infty$ case, this is the MP2 method, we should obtain the potential similar in shape to the OEP2-sc method,[172] which slightly overestimates the reference one. The opposite trend is observed when the calculations are performed in the full KS framework[162,163] (see Figures S1 and S3 in the Supporting Information[147]). The fully local potential affect also the unoccupied KS orbitals what in general have a large impact on the functional performance (see the discussion in this context in Sec 4.1. of ref 163). The increasing percentage of EXX and MP2 leads to increasing discrepancies between the OEP DH v_c and the one obtained from CCSD(T) density. In this case, for $m = \infty$, we will recover the OEP-GL2 method, which, as it is generally known,[165,170,172−176] significantly overestimates correlation effects. This indicates that the full KS realization of DH functionals might lead to a quite different behavior (trends) for systems from Table 3.

In Figures 6 and 7, we report the correlation densities, which support the correlation potential analysis. Also here, PBE0-DH DFA gives almost the same behavior as PBE-QIDH (m = 2) except the core region where it exhibits larger overestimation. This can be simply explained by the larger percentage of exchange DFA mixed in the PBE0-DH functional. Almost the same behavior is observed for the RSX-QIDH density (in the case of RS hybrids), which agrees quite nicely with LRC-ωPBE-DH (m = 2) data. With increasing m, we observe an improvement of densities also in the core region where nonphysical oscillations (inherited from GGA terms[176]) start to be less pronounced. Thus, for m = 4, the agreement with the reference CCSD(T) densities is much better. This analysis somehow also confirms the findings from ref 177 where it was shown that the accuracy of the PBE-based DH densities increases with the amount of EXX and MP2 terms included in the functional (PBE0-DH > PBE-QIDH > PBE0-2 > PBE-

https://dx.doi.org/10.1021/acs.jctc.0c00823
J. Chem. Theory Comput. 2020, 16, 7413−7430

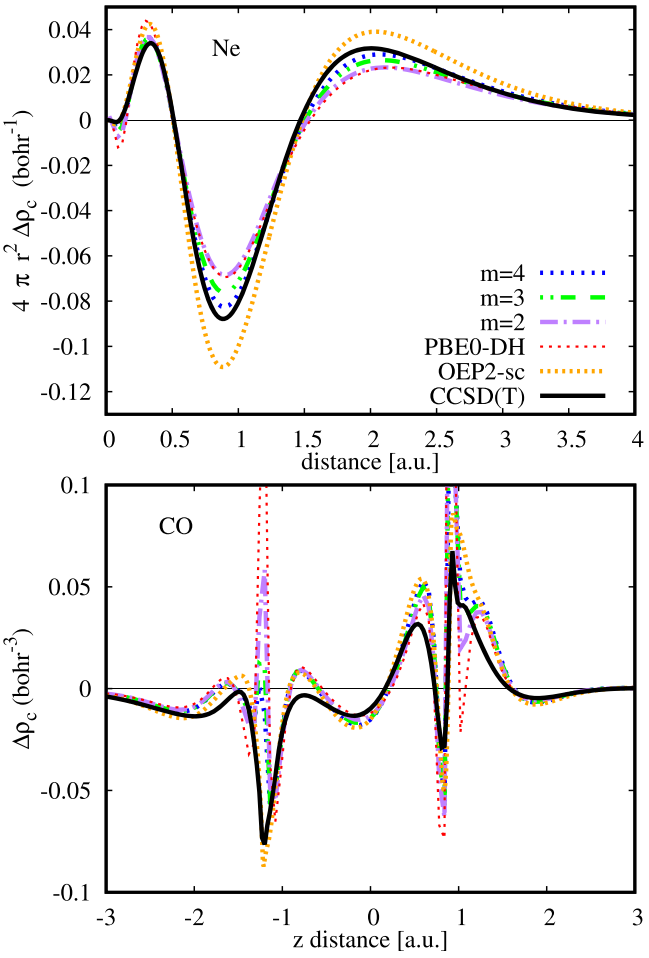

Figure 6. Correlation densities, $\Delta\rho_c = \rho^{method} - \rho^{EXX}$, of the Ne atom (uncontracted ROOS-ATZP[160]) and CO molecule (uncontracted cc-pVTZ,[149] R_0 = 1.128Å) for various PBE-mIDH methods (m = 2 (PBE-QIDX), m = 3 (PBE0-2), and m = 4). The reference CCSD(T) correlation density was calculated with respect to HF density as $\Delta\rho_c = \rho^{CCSD(T)} - \rho^{HF}$ using the same computational setup.

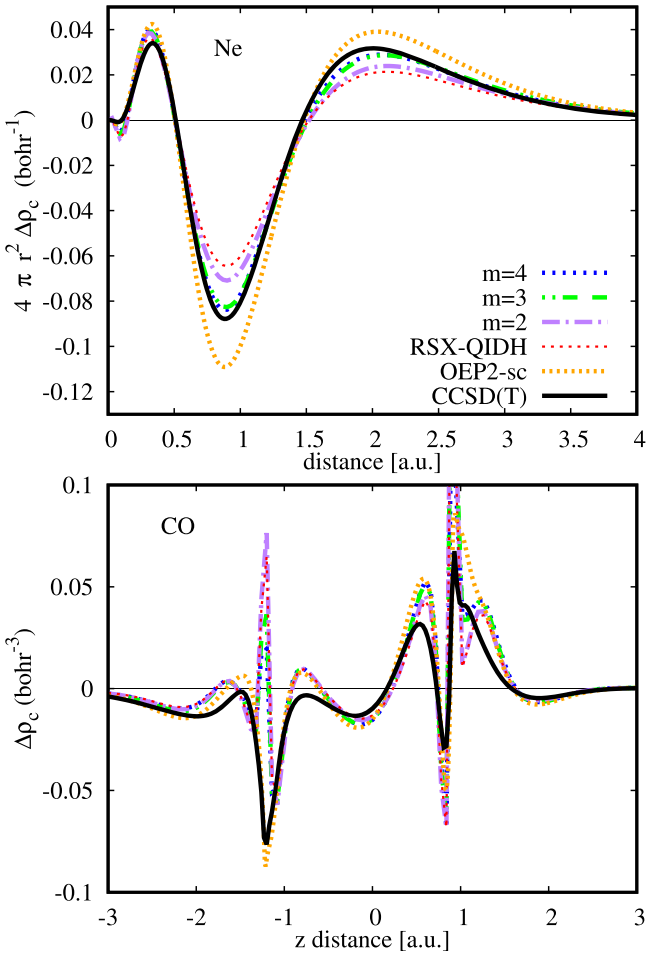

Figure 7. Similar as in Figure 6, but for the LRC-ωPBE-DH (m = 2,3,4) family of functionals.

mIDH (m = 4)). As previously, the full self-consisted KS densities (see Figs. S2 and S4 in ref 147) lead to an opposite trend, and thus the better agreement with reference is obtained for m = 2. The larger the m, the bigger contribution comes from the GL2 term, which leads to an overestimation of correlation effects. This might indicate that DH functionals can benefit from the utilization of orbitals obtained within the GKS framework.

3.2.4. Ionization Potentials. In Figure 8, we report the mean absolute relative errors (MARE) for VIP calculated in two manners: (i) using total energies of neutral and ionic species VIP = E(N) − E(N − 1); (ii) as VIP = − ε_{HOMO} what is directly related with the quality of the XC potential[148,169−171,176,178] (see Section 5 for more details). We note that, for exact DFT calculations, the two computed quantities should be identical.

Let us first turn our attention to the results obtained as energy differences. In this case, all the methods perform quite similarly, giving MAREs in the range of 1.19%−2.77%. The best results are obtained by the PBE-QIDH (m = 2) functional with a MARE of 1.19%, closely followed by the OEP2-sc method (MARE = 1.27%). Surprisingly, the RSX-QIDH functional gives here slightly worse performance with a MARE of 1.62% (see also the G21IP results in Table. 2). The worst VIP is provided by PBE0-DH (MARE of 2.77%) DFA. With increasing of m parameter, we

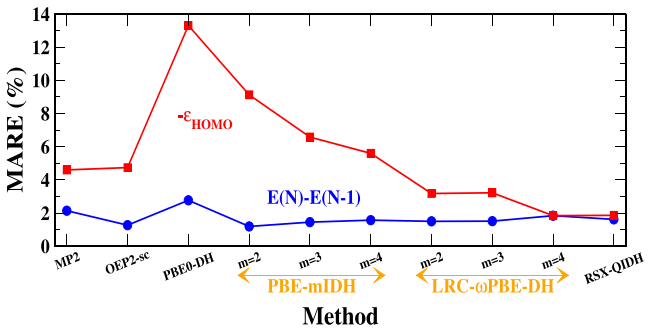

Figure 8. Mean absolute relative errors (MAREs) calculated with respect to CCSD(T), computed with different methods for the vertical ionization potentials of several atoms and molecules. The systems are listed in Table S1 of ref 148. The MP2 and OEP2-sc results are taken from ref 148.

also observe an increase in MARE for both families of functionals, which for m = ∞ should reach the MP2 results, which display a MARE of 2.1%.

Now let us focus on the VIPs obtained from the opposite of the energy of HOMO. Here, the worst performance is provided by PBE0-DH (MARE = 13.31%) followed by PBE-QIDH, which yields a MARE of 9.13%. These two functionals actually exhibit the worse correlation (and thus XC) potentials reported in Section 3.2.3. As previously, the increase in EXX and MP2 terms leads to the improvement of VIP. For PBE-mIDH (m = 4),

https://dx.doi.org/10.1021/acs.jctc.0c00823
J. Chem. Theory Comput. 2020, 16, 7413−7430

we get a MARE of 5.6%, which is about 0.9−1.0% off the MP2 ($m = \infty$) and OEP2-sc results. These predictions are still quite bad with respect to other second-order approaches such as the OEP2-SOSc[179] method, which for the same VIP set yields a MARE of 1.03% (similar to the state-of-art IP-EOM-CCSD[180,181] method, which gives here a MARE of 1.07%).

In the case of RS DH functionals, we observe a drastic improvement in the quality of HOMO energies. Already for m = 2, the inclusion of the LR EXX term reduced the MARE to 3.18%. Surprisingly, for m = 4, we get a MARE of 1.84%, which is identical with MARE calculated for VIP from energy differences (MAEs in this cases are 0.26 and 0.23 eV for $-\varepsilon_{\mathrm{HOMO}}$ and $E(N) - E(N\text{-}1)$, respectively). This indicates the good quality of both the XC potentials and total energies obtained with these DFAs. Similar to LRC-ωPBE-DH (m = 4) DFA, the RSX-QIDH HOMO energies agree quite nicely with VIP calculated as energy differences, giving here a MARE of 1.86%. This can be justified by the optimization/proper selection of the ω parameter in RSX-QIDH DFA, which, as recently shown,[143] is almost equivalent to optical tuning.[142]

4. CONCLUSIONS

We have introduced a generalized theory of the DH density functional using the AC formalism and higher-order many-body perturbation theory. The flavors of the present construction are quite physical and allow one to construct mH functionals of any order. We have shown that the present generalization recovers already existing DFA, namely, the PBE-QIDH and PBE0-2 functionals for certain choices of the parameter m.

Based on the here developed theory, generalized PBE-mIDH and long-range corrected DH functionals have been investigated. These functionals are applied to well-known molecular test cases, and their performances showed an improvement in many cases compared to other DH functionals. In particular, it has been shown that the constructed PBE-mIDH and long-range DH (mixing a larger amount of HF and MP2 terms with increasing value of m parameter) may offer a guiding tool in other areas where mitigating self-interaction error is important. The constructed functionals may also be attractive from the standpoint of application in time-dependent density functional theory.

As the final reflection, the inclusion of HOT of the many-body perturbation theory such as GL3/MP3 and GL4/MP4 leads in general to the improvement of the results, seen in the here investigated total, atomization, and binding energies. However, the substantial computational cost does not allow us to construct a usable functional with the higher perturbation terms such as triple and quadruple hybrids. Those can be considered in the future development of functional construction.

5. COMPUTATIONAL DETAILS

For molecular properties we consider selection of well-defined test sets from the Minnesota 2.0 and GMTKN55.[182] The test sets are divided into three subsets, namely, main group thermochemistry (MGT), barrier heights (BH), and non-covalent interactions (NCI). For the thermochemistry test set, we consider the following: (1) AE6, atomization energies of 6 molecules;[144,146] (2) G2/148, atomization energies of 148 molecules;[183] (3) G21EA, 25 electron affinities;[182,184] (4) G21IP, 36 ionization potentials;[182,184] (5) PA26, 26 proton affinities;[185−187] (6) BH76RC, 30 reaction energies of the BH76 test;[182] and (7) SIE4×4, 16 single-point self-interaction correction problems.[182] For barrier heights, we consider the following: (1) BH6, 6 barrier heights;[144] (2) HTBH38, 38 hydrogen barrier heights;[144] and (3) NHTBH38, 38 non-hydrogen barrier heights.[188] For the non-covalent interaction test set, we consider the following: (1) HB6, 6 hydrogen bond test set;[189] (2) DI6, 6 dipole interactions;[189] (3) CT7, 7 charge transfer molecules;[189] (4) PPS5, 5 $\pi-\pi$ stacking molecules; (5) WI7, 7 weak interaction complexes, bound by dispersion-like interactions;[189] and (6) S22, 22 non-covalent interaction molecules including H-bond, dispersion interactions, and mixed bonds.[190,191] We underline that the here considered test sets represent the overall important chemical properties. Further, we also consider the dissociation energies of H_2^+, He_2^+, and $ArKr^+$ to assess the functional performance. The calculations of all the functionals are performed using the developed version of the Q-CHEM code[192] except the RSX-QIDH functional calculations, which are done in the NWChem package.[193] The def2-QZVP basis set is used for our present calculations, except for the G21EA test set, for which the def2-QZVPD basis set is used. All quantities in this part have been calculated without counterpoise (CP) corrections for the basis set superposition error (BSSE).

Additionally, to assess the accuracy of PBE-mIDH and LRC-ωPBE-DH (m = 2,3,4) family of functionals, we have considered several test cases:

- in Section 3.1, we investigate the impact of higher-order terms (HOT) in eqs 15 and 17 onto the quality of results. In this respect, we define the triple-hybrid (TH) (m = 3, including GL2 and GL3 correlation contributions) and quadruple-hybrid (QH) (m = 4, including GL2, GL3, and GL4 correlation contributions) functionals. In the assessment, we have examined the total energies of several atoms and molecules,[150] interaction energies of a small set of non-covalently bonded molecules from[150] and atomization energies of AE6[144] benchmark set. This is mostly dictated by the substantial computational cost of the inclusion of GL3 and GL4 terms.

  We remark that, because for the HF reference state, the Taylor series around λ = 0 has almost the same small-λ expansion[134] expressed throughout MPk terms; usually in the construction of DH DFAs, one utilized an MP2-like correlation energy expression (the same expression as for the HF theory, but with KS reference orbitals and orbital energies). This is further justified by the small contribution coming from the single excited term (i.e., the last term of eq 9) in the GL2 energy expression.[170] Higher-order GLk energy contribution differ much more from MPk ones (evaluated on the same KS reference state), mostly due to non-vanishing off-diagonal contributions in H_0 (see ref 181 and ref 133 for the diagrammatic representation of third- and fourth-order energy terms). Nevertheless, the dominant energy contribution comes from the MPk-like formula. This is especially valid in our generalized formalism where the HF EXX energy enters the XC expression with at least 66% (HF dominant) contribution. Taking into account that the DH is generally treated within the GKS framework, we expect that the difference between GLn and MPn terms should be rather small. Thus, in the current study, we approximate GL2 and higher-order GLk terms by their MPk counterparts, namely, GL2 ≈ MP2, GL3 ≈ MP3, GL4 ≈ MP4, etc.

https://dx.doi.org/10.1021/acs.jctc.0c00823
J. Chem. Theory Comput. 2020, 16, 7413−7430

The calculations in Section 3.1 have been carried out within the GKS framework using the NWChem package.[193] All interaction energies have been calculated with counterpoise (CP) corrections to remove the basis set superposition error (BSSE).

- using the formalism developed in refs 162. and 163 we have computed the correlation potentials for the Ne atom and CO molecule (see Section 3.2.3). Due to the explicit orbital dependence of EXX and GL2 energy terms, the corresponding correlation potential ($v_c(\mathbf{r}) = \delta E_c[\rho]/\delta\rho(\mathbf{r})$) was computed using the optimized effective potential (OEP) formalism in a post-SCF fashion for fixed reference orbitals, orbital energies, and densities coming from generalized KS (GKS)[194,195] calculations in a one-step procedure.[161] Because eqs 15 and 17, mix semilocal DFAs with WFT energy expressions, in the following, we define the DH correlation functionals as

$$E_c = E_{xc} - E_x^{EXX} \tag{19}$$

We note that a similar approach was already successfully used in several studies[161,171,178,196−198] to investigate the most relevant features of functional derivatives. As shown in ref 161, the behavior of correlation potential depends on the reference orbitals utilized in a one-step procedure. Therefore, the correlation potentials might be considered as a first indicator of the quality of GKS orbitals and densities. Additionally, for comparison, in ref 147, we report the full self-consisted OEP correlation potentials obtained using the formalism developed in ref 162 and taking into account all functional derivative terms. Likewise, in our previous studies,[148,168,170,171,179] in order to solve the OEP equations, we have employed the finite-basis set procedure from refs 199 and 200.

In the same section, we report correlation densities[170,172,176,201,202] defined as

$$\Delta\rho_c = \rho^{method} - \rho^{xref}$$

where ρ^{xref} is the density obtained for the exact exchange only (OEPx)[200,203] (xref = *EXX*) and HF (xref = *HF*) calculations for DFT and conventional WFT methods, respectively. We underline, however, that for all investigated cases, the difference between HF and EXX densities is very small (see, e.g., Fig. S4 in ref 169); thus, the mutual comparison is consistent. In the case of DH DFAs, the ρ^{method} was obtained as follows. As one knows in the DH GKS scheme, the KS equations are solved with disregarded v_c^{MP2} contribution. This means that the self-consistent density does not take into account the orbital relaxation due to this missing correlation term. However, using the converged GKS orbitals, we can include the missing contribution describing this effect. The re-scaled MP2 part[204] can be obtained in a post-SCF fashion from the relaxed MP2 density matrices[205−207] constructed using the Lagrangian approach.[208−210] In principle, the corrected DH density (ρ^{method}) should allow to generate via one of the inverse methods (e.g., the WY method[164]) the same correlation potentials as the one obtained via the one-step procedure. We note that a similar strategy is adopted within the orbital-optimized DH framework[211,212] or EKT-DH[213] method to include the effect of missing second-order contribution. As previously, the full self-consistent OEP results are reported in ref 147.

To compare our results, we have utilized the CCSD(T) correlation densities obtained from the relaxed density matrices[205−207] constructed using the Lagrangian approach.[208−210] The reference correlation potential have been obtained using the method from ref 164 taking as a starting point the relaxed CCSD(T) densities. All calculations have been carried out with a locally modified version of the ACES II[214] program. The Ne and CO OEP calculations have been performed in fully uncontracted ROOS-ATZP[160] and cc-pVTZ[149] basis sets, respectively. For more technical details, we refer the reader to refs 170 and 172.

- as in ref 148, we have obtained the vertical ionization potentials (VIP)[179] for several atoms and molecules computed in two manners: (i) as the energy difference between the neutral and the ionic species[215] (VIP = E(N) − E(N − 1)); (ii) the opposite of energy of the highest occupied molecular orbital (HOMO) (VIP = $-\varepsilon_{HOMO}$). In the case of DH, the HOMO energies are calculated as in refs148, 162, and 163, where the second-order self-energy correction[133] is calculated in a post-SCF fashion on top of GKS DH orbitals (likewise for HF orbitals[215,216]). Like in ref 148, we did not take into account the additional orbital relaxation term due to the second-order correlation; however, as pointed out in ref 217, this contribution should be rather small. The computational setup, namely, basis sets and molecular geometries are identical as in ref 179 (for more details, see Section 3.2.4). The calculations have been performed with a locally modified version of PSI4 quantum chemistry packages.[218]

■ ASSOCIATED CONTENT

Supporting Information

The Supporting Information is available free of charge at https://pubs.acs.org/doi/10.1021/acs.jctc.0c00823.

Total energies, binding energies, atomization energies, and correlation potentials and densities (PDF)

■ AUTHOR INFORMATION

Corresponding Authors

Subrata Jana − *School of Physical Sciences, National Institute of Science Education and Research, HBNI, Bhubaneswar 752050, India;* orcid.org/0000-0002-3736-1948; Email: subrata.jana@niser.ac.in, subrata.niser@gmail.com

Szymon Śmiga − *Institute of Physics, Faculty of Physics, Astronomy and Informatics, Nicolaus Copernicus University, 87-100 Toruń, Poland;* orcid.org/0000-0002-5941-5409; Email: szsmiga@fizyka.umk.pl

Lucian A. Constantin − *Consiglio Nazionale delle Ricerche CNR-NANO, Istituto di Nanoscienze, 41125 Modena, Italy;* orcid.org/0000-0001-8923-3203; Email: lucian.constantin.68@gmail.com

Prasanjit Samal − *School of Physical Sciences, National Institute of Science Education and Research, HBNI, Bhubaneswar 752050, India;* orcid.org/0000-0002-0234-8831; Email: psamal@niser.ac.in

Complete contact information is available at: https://pubs.acs.org/10.1021/acs.jctc.0c00823

https://dx.doi.org/10.1021/acs.jctc.0c00823
J. Chem. Theory Comput. 2020, 16, 7413−7430

Author Contributions

[§]S.J. and S.Ś. contributed equally to this work.

Notes

The authors declare no competing financial interest.

■ ACKNOWLEDGMENTS

S.Ś. is grateful to the Polish National Science Center for the partial financial support under grant no. 2016/21/D/ST4/00903. S.J. is grateful to the NISER for partial financial support. Q-CHEM simulations have been performed on the *KALINGA* and *NISERDFT* high-performance computing facility at NISER, Bhubaneswar. P.S. and S.J. would like to thank Q-Chem, Inc. and developers for providing the source code.

■ REFERENCES

(1) Kohn, W.; Sham, L. J. Self-consistent equations including exchange and correlation effects. *Phys. Rev.* **1965**, *140*, A1133.
(2) Hohenberg, P.; Kohn, W. Inhomogeneous electron gas. *Phys. Rev.* **1964**, *136*, B864.
(3) Burke, K. Perspective on density functional theory. *J. Chem. Phys.* **2012**, *136*, 150901.
(4) Levy, M. On the simple constrained-search reformulation of the Hohenberg−Kohn theorem to include degeneracies and more (1964−1979). *Int. J. Quantum Chem.* **2010**, *110*, 3140−3144.
(5) Levy, M. Mathematical thoughts in DFT. *Int. J. Quantum Chem.* **2016**, *116*, 802−804.
(6) Perdew, J. P.; Burke, K.; Ernzerhof, M. Generalized gradient approximation made simple. *Phys. Rev. Lett.* **1996**, *77*, 3865.
(7) Sun, J.; Ruzsinszky, A.; Perdew, J. P. Strongly constrained and appropriately normed semilocal density functional. *Phys. Rev. Lett.* **2015**, *115*, No. 036402.
(8) Tao, J.; Mo, Y. Accurate semilocal density functional for condensed-matter physics and quantum chemistry. *Phys. Rev. Lett.* **2016**, *117*, No. 073001.
(9) Jana, S.; Sharma, K.; Samal, P. Improving the Performance of Tao-Mo Non-empirical Density Functional with Broader Applicability in Quantum Chemistry and Materials Science. *J. Phys. Chem. A* **2019**, *123*, 6356−6369.
(10) Peverati, R.; Truhlar, D. G. An improved and broadly accurate local approximation to the exchange-correlation density functional: The MN12-L functional for electronic structure calculations in chemistry and physics. *Phys. Chem. Chem. Phys.* **2012**, *14*, 13171−13174.
(11) Peverati, R.; Zhao, Y.; Truhlar, D. G. Generalized Gradient Approximation That Recovers the Second-Order Density-Gradient Expansion with Optimized Across-the-Board Performance. *J. Phys. Chem. Lett.* **2011**, *2*, 1991−1997.
(12) Peverati, R.; Truhlar, D. G. Exchange-Correlation Functional with Good Accuracy for Both Structural and Energetic Properties while Depending Only on the Density and Its Gradient. *J. Chem. Theory Comput.* **2012**, *8*, 2310−2319.
(13) Wang, Y.; Jin, X.; Yu, H. S.; Truhlar, D. G.; He, X. Revised M06-L functional for improved accuracy on chemical reaction barrier heights, noncovalent interactions, and solid-state physics. *PNAS* **2017**, *114*, 8487−8492.
(14) Levy, M.; Perdew, J. P. Hellmann-Feynman, virial, and scaling requisites for the exact universal density functionals. Shape of the correlation potential and diamagnetic susceptibility for atoms. *Phys. Rev. A* **1985**, *32*, 2010.
(15) Görling, A.; Levy, M. Requirements for correlation energy density functionals from coordinate transformations. *Phys. Rev. A* **1992**, *45*, 1509.
(16) Fabiano, E.; Constantin, L. A. Relevance of coordinate and particle-number scaling in density-functional theory. *Phys. Rev. A* **2013**, *87*, No. 012511.
(17) Svendsen, P.-S.; von Barth, U. Gradient expansion of the exchange energy from second-order density response theory. *Phys. Rev. B* **1996**, *54*, 17402.
(18) Antoniewicz, P. R.; Kleinman, L. Kohn-Sham exchange potential exact to first order in ρ (K)/ ρ 0. *Phys. Rev. B* **1985**, *31*, 6779.
(19) Hu, C. D.; Langreth, D. C. Beyond the random-phase approximation in nonlocal-density-functional theory. *Phys. Rev. B* **1986**, *33*, 943.
(20) Ma, S.-K.; Brueckner, K. A. Correlation energy of an electron gas with a slowly varying high density. *Phys. Rev.* **1968**, *165*, 18.
(21) Elliott, P.; Burke, K. Non-empirical derivation of the parameter in the B88 exchange functional. *Can. J. Chem.* **2009**, *87*, 1485−1491.
(22) Elliott, P.; Lee, D.; Cangi, A.; Burke, K. Semiclassical origins of density functionals. *Phys. Rev. Lett.* **2008**, *100*, 256406.
(23) Görling, A.; Levy, M. Exact Kohn-Sham scheme based on perturbation theory. *Phys. Rev. A* **1994**, *50*, 196.
(24) Görling, A.; Levy, M. Correlation-energy functional and its high-density limit obtained from a coupling-constant perturbation expansion. *Phys. Rev. B* **1993**, *47*, 13105.
(25) Görling, A.; Levy, M. Hardness of molecules and the band gap of solids within the Kohn-Sham formalism: A perturbation-scaling approach. *Phys. Rev. A* **1995**, *52*, 4493.
(26) Della Sala, F.; Görling, A. Asymptotic behavior of the Kohn-Sham exchange potential. *Phys. Rev. Lett.* **2002**, *89*, No. 033003.
(27) Engel, E.; Chevary, J.; Macdonald, L.; Vosko, S. Asymptotic properties of the exchange energy density and the exchange potential of finite systems: relevance for generalized gradient approximations. *Z. Phys. D* **1992**, *23*, 7−14.
(28) Horowitz, C. M.; Constantin, L. A.; Proetto, C. R.; Pitarke, J. M. Position-dependent exact-exchange energy for slabs and semi-infinite jellium. *Phys. Rev. B* **2009**, *80*, 235101.
(29) Constantin, L. A.; Pitarke, J. M. Adiabatic-connection-fluctuation-dissipation approach to long-range behavior of exchange-correlation energy at metal surfaces: A numerical study for jellium slabs. *Phys. Rev. B* **2011**, *83*, No. 075116.
(30) Constantin, L. A.; Fabiano, E.; Pitarke, J. M.; Della Sala, F. Semilocal density functional theory with correct surface asymptotics. *Phys. Rev. B* **2016**, *93*, 115127.
(31) Niquet, Y. M.; Fuchs, M.; Gonze, X. Asymptotic behavior of the exchange-correlation potentials from the linear-response Sham−Schlüter equation. *J. Chem. Phys.* **2003**, *118*, 9504−9518.
(32) Almbladh, C.-O.; von Barth, U. Exact results for the charge and spin densities, exchange-correlation potentials, and density-functional eigenvalues. *Phys. Rev. B* **1985**, *31*, 3231.
(33) Umrigar, C. J.; Gonze, X. Accurate exchange-correlation potentials and total-energy components for the helium isoelectronic series. *Phys. Rev. A* **1994**, *50*, 3827.
(34) Pollack, L.; Perdew, J. P. Evaluating density functional performance for the quasi-two-dimensional electron gas. *J. Phys. Condens. Matter.* **2000**, *12*, 1239.
(35) Kaplan, A. D.; Wagle, K.; Perdew, J. P. Collapse of the electron gas from three to two dimensions in Kohn-Sham density functional theory. *Phys. Rev. B* **2018**, *98*, No. 085147.
(36) Constantin, L. A. Simple effective interaction for dimensional crossover. *Phys. Rev. B* **2016**, *93*, 121104.
(37) Constantin, L. A. Correlation energy functionals from adiabatic connection formalism. *Phys. Rev. B* **2019**, *99*, No. 085117.
(38) Lieb, E. H.; Oxford, S. Improved lower bound on the indirect Coulomb energy. *Int. J. Quantum Chem.* **1981**, *19*, 427−439.
(39) Seidl, M.; Vuckovic, S.; Gori-Giorgi, P. Challenging the Lieb−Oxford bound in a systematic way. *Mol. Phys.* **2016**, *114*, 1076−1085.
(40) Constantin, L. A.; Terentjevs, A.; Della Sala, F.; Fabiano, E. Gradient-dependent upper bound for the exchange-correlation energy and application to density functional theory. *Phys. Rev. B* **2015**, *91*, No. 041120.
(41) Vuckovic, S.; Irons, T. J. P.; Wagner, L. O.; Teale, A. M.; Gori-Giorgi, P. Interpolated energy densities, correlation indicators and lower bounds from approximations to the strong coupling limit of DFT. *Phys. Chem. Chem. Phys.* **2017**, *19*, 6169−6183.

https://dx.doi.org/10.1021/acs.jctc.0c00823
J. Chem. Theory Comput. 2020, 16, 7413−7430

(42) Perdew, J. P.; Ruzsinszky, A.; Sun, J.; Burke, K. Gedanken densities and exact constraints in density functional theory. *J. Chem. Phys.* **2014**, *140*, 18A533.
(43) Lewin, M.; Lieb, E. H. Improved Lieb-Oxford exchange-correlation inequality with a gradient correction. *Phys. Rev. A* **2015**, *91*, No. 022507.
(44) Feinblum, D. V.; Kenison, J.; Burke, K. Communication: Testing and using the Lewin-Lieb bounds in density functional theory. *J. Chem. Phys.* **2014**, *141*, 241105.
(45) Tao, J.; Staroverov, V. N.; Scuseria, G. E.; Perdew, J. P. Exact-exchange energy density in the gauge of a semilocal density-functional approximation. *Phys. Rev. A* **2008**, *77*, No. 012509.
(46) Přecechtělová, J.; Bahmann, H.; Kaupp, M.; Ernzerhof, M. Communication: A non-empirical correlation factor model for the exchange-correlation energy. *J. Chem. Phys.* **2014**, *141*, 111102.
(47) Přecechtělová, J. P.; Bahmann, H.; Kaupp, M.; Ernzerhof, M. Design of exchange-correlation functionals through the correlation factor approach. *J. Chem. Phys.* **2015**, *143*, 144102.
(48) Perdew, J. P.; Schmidt, K. Jacob's ladder of density functional approximations for the exchange-correlation energy. *AIP Conf. Proc.* **2001**, 1−20.
(49) Scuseria, G. E.; Staroverov, V. N. Progress in the development of exchange-correlation functionals. In *Theory and Application of Computational Chemistry: The First 40 Years*; Dykstra, C. E., Frenking, G., Kim, K. S., Scuseria, G. E., Eds.; Elsevier: Amsterdam, 2005; pp. 669−724.
(50) Della Sala, F.; Fabiano, E.; Constantin, L. A. Kinetic-energy-density dependent semilocal exchange-correlation functionals. *Int. J. Quantum Chem.* **2016**, *116*, 1641−1694.
(51) Staroverov, V. N.; Scuseria, G. E.; Tao, J.; Perdew, J. P. Comparative assessment of a new nonempirical density functional: Molecules and hydrogen-bonded complexes. *J. Chem. Phys.* **2003**, *119*, 12129−12137.
(52) Mo, Y.; Tian, G.; Tao, J. Performance of a nonempirical exchange functional from density matrix expansion: comparative study with different correlations. *Phys. Chem. Chem. Phys.* **2017**, *19*, 21707−21713.
(53) Tran, F.; Stelzl, J.; Blaha, P. Rungs 1 to 4 of DFT Jacob's ladder: Extensive test on the lattice constant, bulk modulus, and cohesive energy of solids. *J. Chem. Phys.* **2016**, *144*, 204120.
(54) Haas, P.; Tran, F.; Blaha, P. Calculation of the lattice constant of solids with semilocal functionals. *Phys. Rev. B* **2009**, *79*, No. 085104.
(55) Lejaeghere, K.; et al. Reproducibility in density functional theory calculations of solids. *Science* **2016**, *351*, aad3000.
(56) Mo, Y.; Tian, G.; Tao, J. Comparative study of semilocal density functionals on solids and surfaces. *Chem. Phys. Lett.* **2017**, *682*, 38−42.
(57) Mo, Y.; Car, R.; Staroverov, V. N.; Scuseria, G. E.; Tao, J. Assessment of the Tao-Mo nonempirical semilocal density functional in applications to solids and surfaces. *Phys. Rev. B* **2017**, *95*, No. 035118.
(58) Jana, S.; Patra, A.; Samal, P. Assessing the performance of the Tao-Mo semilocal density functional in the projector-augmented-wave method. *J. Chem. Phys.* **2018**, *149*, No. 044120.
(59) Jana, S.; Sharma, K.; Samal, P. Assessing the performance of the recent meta-GGA density functionals for describing the lattice constants, bulk moduli, and cohesive energies of alkali, alkaline-earth, and transition metals. *J. Chem. Phys.* **2018**, *149*, 164703.
(60) Patra, B.; Jana, S.; Constantin, L. A.; Samal, P. Relevance of the Pauli kinetic energy density for semilocal functionals. *Phys. Rev. B* **2019**, *100*, 155140.
(61) Patra, A.; Patra, B.; Constantin, L. A.; Samal, P. Electronic band structure of layers within meta generalized gradient approximation of density functionals. *Phys. Rev. B* **2020**, *102*, No. 045135.
(62) Grimme, S. Semiempirical hybrid density functional with perturbative second-order correlation. *J. Chem. Phys.* **2006**, *124*, No. 034108.
(63) Becke, A. D. A new mixing of Hartree-Fock and local density-functional theories. *J. Chem. Phys.* **1993**, *98*, 1372−1377.
(64) Stephens, P. J.; Devlin, F. J.; Chabalowski, C. F.; Frisch, M. J. Ab Initio Calculation of Vibrational Absorption and Circular Dichroism Spectra Using Density Functional Force Fields. *J. Phys. Chem. A* **1994**, *98*, 11623−11627.
(65) Ernzerhof, M.; Scuseria, G. E. Assessment of the Perdew−Burke−Ernzerhof exchange-correlation functional. *J. Chem. Phys.* **1999**, *110*, 5029−5036.
(66) Wilson, P. J.; Bradley, T. J.; Tozer, D. J. Hybrid exchange-correlation functional determined from thermochemical data and ab initio potentials. *J. Chem. Phys.* **2001**, *115*, 9233−9242.
(67) Keal, T. W.; Tozer, D. J. Semiempirical hybrid functional with improved performance in an extensive chemical assessment. *J. Chem. Phys.* **2005**, *123*, 121103.
(68) Boese, A. D.; Martin, J. M. L. Development of density functionals for thermochemical kinetics. *J. Chem. Phys.* **2004**, *121*, 3405−3416.
(69) Lynch, B. J.; Fast, P. L.; Harris, M.; Truhlar, D. G. Adiabatic Connection for Kinetics. *J. Phys. Chem. A* **2000**, *104*, 4811−4815.
(70) Peverati, R.; Truhlar, D. G. Communication: A global hybrid generalized gradient approximation to the exchange-correlation functional that satisfies the second-order density-gradient constraint and has broad applicability in chemistry. *J. Chem. Phys.* **2011**, *135*, 191102.
(71) Xu, X.; Goddard, W. A. The X3LYP extended density functional for accurate descriptions of nonbond interactions, spin states, and thermochemical properties. *PNAS* **2004**, *101*, 2673−2677.
(72) Zhao, Y.; Truhlar, D. G. The M06 suite of density functionals for main group thermochemistry, thermochemical kinetics, noncovalent interactions, excited states, and transition elements: two new functionals and systematic testing of four M06-class functionals and 12 other functionals. *Theor. Chem. Acc.* **2008**, *120*, 215−241.
(73) Csonka, G. I.; Perdew, J. P.; Ruzsinszky, A. Global hybrid functionals: A look at the engine under the hood. *J. Chem. Theory Comput.* **2010**, *6*, 3688−3703.
(74) Adamo, C.; Barone, V. Toward reliable density functional methods without adjustable parameters: The PBE0 model. *J. Chem. Phys.* **1999**, *110*, 6158−6170.
(75) Zhao, Y.; Lynch, B. J.; Truhlar, D. G. Doubly Hybrid Meta DFT: New Multi-Coefficient Correlation and Density Functional Methods for Thermochemistry and Thermochemical Kinetics. *J. Phys. Chem. A* **2004**, *108*, 4786−4791.
(76) Yu, H. S.; He, X.; Li, S. L.; Truhlar, D. G. MN15: A Kohn-Sham global-hybrid exchange-correlation density functional with broad accuracy for multi-reference and single-reference systems and non-covalent interactions. *Chem. Sci.* **2016**, *7*, 5032−5051.
(77) Hui, K.; Chai, J.-D. SCAN-based hybrid and double-hybrid density functionals from models without fitted parameters. *J. Chem. Phys.* **2016**, *144*, No. 044114.
(78) Zhao, Y.; Truhlar, D. G. Hybrid Meta Density Functional Theory Methods for Thermochemistry, Thermochemical Kinetics, and Non-covalent Interactions: The MPW1B95 and MPWB1K Models and Comparative Assessments for Hydrogen Bonding and van der Waals Interactions. *J. Phys. Chem. A* **2004**, *108*, 6908−6918.
(79) Gerosa, M.; Bottani, C. E.; Caramella, L.; Onida, G.; Di Valentin, C.; Pacchioni, G. Electronic structure and phase stability of oxide semiconductors: Performance of dielectric-dependent hybrid functional DFT, benchmarked against G W band structure calculations and experiments. *Phys. Rev. B* **2015**, *91*, 155201.
(80) Brawand, N. P.; Vörös, M.; Govoni, M.; Galli, G. Generalization of dielectric-dependent hybrid functionals to finite systems. *Phys. Rev. X* **2016**, *6*, No. 041002.
(81) Fabiano, E.; Constantin, L. A.; Della Sala, F. Testing the broad applicability of the PBEint GGA functional and its one-parameter hybrid form. *Int. J. Quantum Chem.* **2013**, *113*, 673−682.
(82) Fabiano, E.; Constantin, L. A.; Cortona, P.; Della Sala, F. Global hybrids from the semiclassical atom theory satisfying the local density linear response. *J. Chem. Theory Comput.* **2014**, *11*, 122−131.
(83) Møller, C.; Plesset, M. S. Note on an approximate treatment for many-electron systems. *Phys. Rev.* **1934**, *36*, 618−622.
(84) Goerigk, L.; Grimme, S. Double-hybrid density functionals. *WIREs Comput. Mol. Sci.* **2014**, *4*, 576−600.

https://dx.doi.org/10.1021/acs.jctc.0c00823
J. Chem. Theory Comput. 2020, 16, 7413−7430

(85) Mehta, N.; Casanova-Páez, M.; Goerigk, L. Semi-empirical or non-empirical double-hybrid density functionals: which are more robust? *Phys. Chem. Chem. Phys.* **2018**, *20*, 23175−23194.
(86) Mardirossian, N.; Head-Gordon, M. B97X-V: A 10-parameter, range-separated hybrid, generalized gradient approximation density functional with nonlocal correlation, designed by a survival-of-the-fittest strategy. *Phys. Chem. Chem. Phys.* **2014**, *16*, 9904−9924.
(87) Lin, Y.-S.; Li, G.-D.; Mao, S.-P.; Chai, J.-D. Long-Range Corrected Hybrid Density Functionals with Improved Dispersion Corrections. *J. Chem. Theory Comput.* **2013**, *9*, 263−272.
(88) Chai, J.-D.; Head-Gordon, M. Long-range corrected hybrid density functionals with damped atom-atom dispersion corrections. *Phys. Chem. Chem. Phys.* **2008**, *10*, 6615−6620.
(89) Yanai, T.; Tew, D. P.; Handy, N. C. A new hybrid exchange-correlation functional using the Coulomb-attenuating method (CAM-B3LYP). *Chem. Phys. Lett.* **2004**, *393*, 51−57.
(90) Verma, P.; Bartlett, R. J. Increasing the applicability of density functional theory. IV. Consequences of ionization-potential improved exchange-correlation potentials. *J. Chem. Phys.* **2014**, *140*, 18A534.
(91) Henderson, T. M.; Izmaylov, A. F.; Scuseria, G. E.; Savin, A. Assessment of a middle-range hybrid functional. *J. Chem. Theory Comput.* **2008**, *4*, 1254−1262.
(92) Weintraub, E.; Henderson, T. M.; Scuseria, G. E. Long-Range-Corrected Hybrids Based on a New Model Exchange Hole. *J. Chem. Theory Comput.* **2009**, *5*, 754−762 26609580.
(93) Peverati, R.; Truhlar, D. G. Screened-exchange density functionals with broad accuracy for chemistry and solid-state physics. *Phys. Chem. Chem. Phys.* **2012**, *14*, 16187−16191.
(94) Rohrdanz, M. A.; Martins, K. M.; Herbert, J. M. A long-range-corrected density functional that performs well for both ground-state properties and time-dependent density functional theory excitation energies, including charge-transfer excited states. *J. Chem. Phys.* **2009**, *130*, No. 054112.
(95) Chai, J.-D.; Head-Gordon, M. Systematic optimization of long-range corrected hybrid density functionals. *J. Chem. Phys.* **2008**, *128*, No. 084106.
(96) Tao, J.; Bulik, I. W.; Scuseria, G. E. Semilocal exchange hole with an application to range-separated density functionals. *Phys. Rev. B* **2017**, *95*, 125115.
(97) Patra, B.; Jana, S.; Samal, P. Long-range corrected density functional through the density matrix expansion based semilocal exchange hole. *Phys. Chem. Chem. Phys.* **2018**, *20*, 8991−8998.
(98) Jana, S.; Samal, P. A meta-GGA level screened range-separated hybrid functional by employing short range Hartree-Fock with a long range semilocal functional. *Phys. Chem. Chem. Phys.* **2018**, *20*, 8999−9005.
(99) Vydrov, O. A.; Heyd, J.; Krukau, A. V.; Scuseria, G. E. Importance of short-range versus long-range Hartree-Fock exchange for the performance of hybrid density functionals. *J. Chem. Phys.* **2006**, *125*, No. 074106.
(100) Toulouse, J.; Colonna, F.; Savin, A. Short-range exchange and correlation energy density functionals: Beyond the local-density approximation. *J. Chem. Phys.* **2005**, *122*, No. 014110.
(101) Stoyanova, A.; Teale, A. M.; Toulouse, J.; Helgaker, T.; Fromager, E. Alternative separation of exchange and correlation energies in multi-configuration range-separated density-functional theory. *J. Chem. Phys.* **2013**, *139*, 134113.
(102) Toulouse, J.; Savin, A. Local density approximation for long-range or for short-range energy functionals? *J. Mol. Struct.* **2006**, *762*, 147−150. , A Collection of Papers Dedicated to Professor Annick Goursot on the Occasion of her 60th Birthday.
(103) Sansone, G.; Civalleri, B.; Usvyat, D.; Toulouse, J.; Sharkas, K.; Maschio, L. Range-separated double-hybrid density-functional theory applied to periodic systems. *J. Chem. Phys.* **2015**, *143*, 102811.
(104) Kalai, C.; Toulouse, J. A general range-separated double-hybrid density-functional theory. *J. Chem. Phys.* **2018**, *148*, 164105.
(105) Toulouse, J.; Savin, A.; Flad, H.-J. Short-range exchange-correlation energy of a uniform electron gas with modified electron−electron interaction. *Int. J. Quantum Chem.* **2004**, *100*, 1047−1056.
(106) Gerber, I. C.; Angyán, J. G. Hybrid functional with separated range. *Chem. Phys. Lett.* **2005**, *415*, 100−105.
(107) Henderson, T. M.; Izmaylov, A. F.; Scalmani, G.; Scuseria, G. E. Can short-range hybrids describe long-range-dependent properties? *J. Chem. Phys.* **2009**, *131*, No. 044108.
(108) Song, J.-W.; Tokura, S.; Sato, T.; Watson, M. A.; Hirao, K. An improved long-range corrected hybrid exchange-correlation functional including a short-range Gaussian attenuation (LCgau-BOP). *J. Chem. Phys.* **2007**, *127*, 154109.
(109) Krukau, A. V.; Scuseria, G. E.; Perdew, J. P.; Savin, A. Hybrid functionals with local range separation. *J. Chem. Phys.* **2008**, *129*, 124103.
(110) Toulouse, J.; Gerber, I. C.; Jansen, G.; Savin, A.; Ángyán, J. G. Adiabatic-Connection Fluctuation-Dissipation Density-Functional Theory Based on Range Separation. *Phys. Rev. Lett.* **2009**, *102*, No. 096404.
(111) Chermak, E.; Mussard, B.; Ángyán, J. G.; Reinhardt, P. Short range DFT combined with long-range local RPA within a range-separated hybrid DFT framework. *Chem. Phys. Lett.* **2012**, *550*, 162−169.
(112) Henderson, T. M.; Janesko, B. G.; Scuseria, G. E.; Savin, A. Locally range-separated hybrids as linear combinations of range-separated local hybrids. *Int. J. Quantum Chem.* **2009**, *109*, 2023−2032.
(113) Heyd, J.; Scuseria, G. E.; Ernzerhof, M. Hybrid functionals based on a screened Coulomb potential. *J. Chem. Phys.* **2003**, *118*, 8207−8215.
(114) Toulouse, J.; Gori-Giorgi, P.; Savin, A. Scaling relations, virial theorem, and energy densities for long-range and short-range density functionals. *Int. J. Quantum Chem.* **2006**, *106*, 2026−2034.
(115) Janesko, B. G.; Henderson, T. M.; Scuseria, G. E. Long-range-corrected hybrid density functionals including random phase approximation correlation: Application to noncovalent interactions. *J. Chem. Phys.* **2009**, *131*, No. 034110.
(116) Heyd, J.; Scuseria, G. E. Efficient hybrid density functional calculations in solids: Assessment of the Heyd−Scuseria−Ernzerhof screened Coulomb hybrid functional. *J. Chem. Phys.* **2004**, *121*, 1187−1192.
(117) Paier, J.; Marsman, M.; Hummer, K.; Kresse, G.; Gerber, I. C.; Ángyán, J. G. Screened hybrid density functionals applied to solids. *J. Chem. Phys.* **2006**, *124*, 154709.
(118) Krukau, A. V.; Vydrov, O. A.; Izmaylov, A. F.; Scuseria, G. E. Influence of the exchange screening parameter on the performance of screened hybrid functionals. *J. Chem. Phys.* **2006**, *125*, 224106.
(119) Jana, S.; Patra, A.; Constantin, L. A.; Myneni, H.; Samal, P. Long-range screened hybrid-functional theory satisfying the local-density linear response. *Phys. Rev. A* **2019**, *99*, No. 042515.
(120) Schimka, L.; Harl, J.; Kresse, G. Improved hybrid functional for solids: The HSEsol functional. *J. Chem. Phys.* **2011**, *134*, No. 024116.
(121) Jana, S.; Patra, B.; Śmiga, S.; Constantin, L. A.; Samal, P. Improved solid stability from a screened range-separated hybrid functional by satisfying semiclassical atom theory and local density linear response. *Phys. Rev. B* **2020**, *102*, 155107.
(122) Jana, S.; Patra, A.; Samal, P. Efficient lattice constants and energy bandgaps for condensed systems from a meta-GGA level screened range-separated hybrid functional. *J. Chem. Phys.* **2018**, *149*, No. 094105.
(123) Sharkas, K.; Toulouse, J.; Savin, A. Double-hybrid density-functional theory made rigorous. *J. Chem. Phys.* **2011**, *134*, No. 064113.
(124) Toulouse, J.; Sharkas, K.; Brémond, E.; Adamo, C. Communication: Rationale for a new class of double-hybrid approximations in density-functional theory. *J. Chem. Phys.* **2011**, *135*, 101102.
(125) Ernzerhof, M. Construction of the adiabatic connection. *Chem. Phys. Lett.* **1996**, *263*, 499−506.
(126) Görling, A. Exact exchange kernel for time-dependent density-functional theory. *Int. J. Quantum Chem.* **1998**, *69*, 265−277.
(127) Alipour, M. Designing a paradigm for parameter-free double-hybrid density functionals through the adiabatic connection path. *Theor. Chem. Acc.* **2015**, *134*, 87.

https://dx.doi.org/10.1021/acs.jctc.0c00823
J. Chem. Theory Comput. 2020, 16, 7413−7430

(128) Grabowski, I.; Lotrich, V.; Hirata, S. Ab initio DFT - the seamless connection between WFT and DFT. *Mol. Phys.* **2010**, *108*, 3313−3322.
(129) Brémond, E.; Adamo, C. Seeking for parameter-free double-hybrid functionals: The PBE0-DH model. *J. Chem. Phys.* **2011**, *135*, No. 024106.
(130) Chai, J.-D.; Mao, S.-P. Seeking for reliable double-hybrid density functionals without fitting parameters: The PBE0-2 functional. *Chem. Phys. Lett.* **2012**, *538*, 121−125.
(131) Brémond, E.; Sancho-García, J. C.; Pérez-Jiménez, Á. J.; Adamo, C. Communication: Double-hybrid functionals from adiabatic-connection: The QIDH model. *J. Chem. Phys.* **2014**, *141*, No. 031101.
(132) Peach, M. J. G.; Teale, A. M.; Tozer, D. J. Modeling the adiabatic connection in H2. *J. Chem. Phys.* **2007**, *126*, 244104.
(133) Szabo, A.; Ostlund, N. S. *Modern Quantum Chemistry: Introduction to Advanced Electronic Structure Theory*; Dover: New York, 1996.
(134) Seidl, M.; Giarrusso, S.; Vuckovic, S.; Fabiano, E.; Gori-Giorgi, P. Communication: Strong-interaction limit of an adiabatic connection in Hartree-Fock theory. *J. Chem. Phys.* **2018**, *149*, 241101.
(135) Seidl, M.; Perdew, J. P.; Kurth, S. Simulation of all-order density-functional perturbation theory, using the second order and the strong-correlation limit. *Phys. Rev. Lett.* **2000**, *84*, 5070.
(136) Manby, F. R.; Knowles, P. J. A perturbation theory using a local potential from Hartree-Fock orbitals. *Chem. Phys. Lett.* **1998**, *296*, 1−7.
(137) Ángyán, J. G.; Gerber, I. C.; Savin, A.; Toulouse, J. van der Waals forces in density functional theory: Perturbational long-range electron-interaction corrections. *Phys. Rev. A* **2005**, *72*, No. 012510.
(138) Chai, J.-D.; Head-Gordon, M. Long-range corrected double-hybrid density functionals. *J. Chem. Phys.* **2009**, *131*, 174105.
(139) Brémond, E.; Pérez-Jiménez, Á. J.; Sancho-García, J. C.; Adamo, C. Range-separated hybrid density functionals made simple. *J. Chem. Phys.* **2019**, *150*, 201102.
(140) Brémond, E.; Savarese, M.; Pérez-Jiménez, Á. J.; Sancho-García, J. C.; Adamo, C. Range-Separated Double-Hybrid Functional from Nonempirical Constraints. *J. Chem. Theory Comput.* **2018**, *14*, 4052−4062 29923721.
(141) Vydrov, O. A.; Scuseria, G. E. Assessment of a long-range corrected hybrid functional. *J. Chem. Phys.* **2006**, *125*, 234109.
(142) Baer, R.; Livshits, E.; Salzner, U. Tuned Range-Separated Hybrids in Density Functional Theory. *Annu. Rev. Phys. Chem.* **2010**, *61*, 85−109 PMID: 20055678.
(143) Brémond, E.; Pérez-Jiménez, Á. J.; Sancho-García, J. C.; Adamo, C. Range-separated hybrid and double-hybrid density functionals: A quest for the determination of the range-separation parameter. *J. Chem. Phys.* **2020**, *152*, 244124.
(144) Lynch, B. J.; Truhlar, D. G. Small Representative Benchmarks for Thermochemical Calculations. *J. Phys. Chem. A* **2004**, *108*, 1460−1460.
(145) Raghavachari, K.; Trucks, G. W.; Pople, J. A.; Head-Gordon, M. A fifth-order perturbation comparison of electron correlation theories. *Chem. Phys. Lett.* **1989**, *157*, 479−483.
(146) Haunschild, R.; Klopper, W. Erratum to: Theoretical reference values for the AE6 and BH6 test sets from explicitly correlated coupled-cluster theory. *Theor. Chem. Acc.* **2013**, *132*, 1306.
(147) Jana, S.; Śmiga, S.; Constantin, L. A.; Samal, P. Supporting Information.
(148) Śmiga, S.; Marusiak, V.; Grabowski, I.; Fabiano, E. The ab initio density functional theory applied for spin-polarized calculations. *J. Chem. Phys.* **2020**, *152*, No. 054109.
(149) Dunning, T. H. Gaussian basis sets for use in correlated molecular calculations. I. The atoms boron through neon and hydrogen. *J. Chem. Phys.* **1989**, *90*, 1007−1023.
(150) Śmiga, S.; Fabiano, E. Approximate solution of coupled cluster equations: application to the coupled cluster doubles method and non-covalent interacting systems. *Phys. Chem. Chem. Phys.* **2017**, *19*, 30249−30260.
(151) Mori-Sánchez, P.; Cohen, A. J.; Yang, W. Many-electron self-interaction error in approximate density functionals. *J. Chem. Phys.* **2006**, *125*, 201102.
(152) Tsuneda, T.; Hirao, K. Self-interaction corrections in density functional theory. *J. Chem. Phys.* **2014**, *140*, 18A513.
(153) Ruzsinszky, A.; Perdew, J. P.; Csonka, G. I.; Vydrov, O. A.; Scuseria, G. E. Spurious fractional charge on dissociated atoms: Pervasive and resilient self-interaction error of common density functionals. *J. Chem. Phys.* **2006**, *125*, 194112.
(154) Ruzsinszky, A.; Perdew, J. P.; Csonka, G. I.; Vydrov, O. A.; Scuseria, G. E. Density functionals that are one- and two- are not always many-electron self-interaction-free, as shown for H2+, He2+, LiH+, and Ne2+. *J. Chem. Phys.* **2007**, *126*, 104102.
(155) Jana, S.; Patra, B.; Myneni, H.; Samal, P. On the many-electron self-interaction error of the semilocal exchange hole based meta-GGA level range-separated hybrid with the B88 hybrids. *Chem. Phys. Lett.* **2018**, *713*, 1−9.
(156) Bao, J. L.; Gagliardi, L.; Truhlar, D. G. Self-Interaction Error in Density Functional Theory: An Appraisal. *J. Phys. Chem. Lett.* **2018**, *9*, 2353−2358.
(157) Cohen, A. J.; Mori-Sanchez, P.; Yang, W. Insights into current limitations of density functional theory. *Science* **2008**, *321*, 792−794.
(158) Constantin, L. A.; Fabiano, E.; Della Sala, F. Hartree potential dependent exchange functional. *J. Chem. Phys.* **2016**, *145*, No. 084110.
(159) Gräfenstein, J.; Kraka, E.; Cremer, D. The impact of the self-interaction error on the density functional theory description of dissociating radical cations: Ionic and covalent dissociation limits. *J. Chem. Phys.* **2004**, *120*, 524−539.
(160) Widmark, P.-O.; Malmqvist, P.-Å.; Roos, B. O. Density matrix averaged atomic natural orbital (ANO) basis sets for correlated molecular wave functions. *Theor. Chim. Acta* **1990**, *77*, 291−306.
(161) Grabowski, I.; Lotrich, V. Accurate orbital-dependent correlation and exchange-correlation potentials from non-iterative ab initio dft calculations. *Mol. Phys.* **2005**, *103*, 2085−2092.
(162) Śmiga, S.; Franck, O.; Mussard, B.; Buksztel, A.; Grabowski, I.; Luppi, E.; Toulouse, J. Self-consistent double-hybrid density-functional theory using the optimized-effective-potential method. *J. Chem. Phys.* **2016**, *145*, 144102.
(163) Śmiga, S.; Grabowski, I.; Witkowski, M.; Mussard, B.; Toulouse, J. Self-Consistent Range-Separated Density-Functional Theory with Second-Order Perturbative Correction via the Optimized-Effective-Potential Method. *J. Chem. Theory Comput.* **2020**, *16*, 211−223.
(164) Wu, Q.; Yang, W. A direct optimization method for calculating density functionals and exchange?correlation potentials from electron densities. *J. Chem. Phys.* **2003**, *118*, 2498−2509.
(165) Bartlett, R. J.; Grabowski, I.; Hirata, S.; Ivanov, S. The exchange-correlation potential in ab initio density functional theory. *J. Chem. Phys.* **2005**, *122*, No. 034104.
(166) Śmiga, S.; Fabiano, E.; Constantin, L. A.; Della Sala, F. Laplacian-dependent models of the kinetic energy density: Applications in subsystem density functional theory with meta-generalized gradient approximation functionals. *J. Chem. Phys.* **2017**, *146*, No. 064105.
(167) Śmiga, S.; Constantin, L. A.; Della Sala, F.; Fabiano, E. The Role of the Reduced Laplacian Renormalization in the Kinetic Energy Functional Development. *Computation* 2019, *7*, DOI: 10.3390/computation7040065.
(168) Buksztel, A.; Śmiga, S.; Grabowski, I. The Correlation Effects in Density Functional Theory Along the Dissociation Path. In *Adv. Quantum Chem.*; Elsevier, 2016; Vol. *73*; pp. 263−283.
(169) Śmiga, S.; Constantin, L. A. Unveiling the Physics Behind Hybrid Functionals. *J. Phys. Chem. A* **2020**, *124*, 5606−5614 PMID: 32551627.
(170) Grabowski, I.; Fabiano, E.; Teale, A. M.; Śmiga, S.; Buksztel, A.; Della Sala, F. Orbital-dependent second-order scaled-opposite-spin correlation functionals in the optimized effective potential method. *J. Chem. Phys.* **2014**, *141*, No. 024113.
(171) Fabiano, E.; Śmiga, S.; Giarrusso, S.; Daas, T. J.; Della Sala, F.; Grabowski, I.; Gori-Giorgi, P. Investigation of the Exchange-Correlation Potentials of Functionals Based on the Adiabatic

Connection Interpolation. *J. Chem. Theory Comput.* **2019**, *15*, 1006−1015.
(172) Grabowski, I.; Teale, A. M.; Śmiga, S.; Bartlett, R. J. Comparing ab initio density-functional and wave function theories: The impact of correlation on the electronic density and the role of the correlation potential. *J. Chem. Phys.* **2011**, *135*, 114111.
(173) Facco Bonetti, A.; Engel, E.; Schmid, R. N.; Dreizler, R. M. Investigation of the Correlation Potential from Kohn-Sham Perturbation Theory. *Phys. Rev. Lett.* **2001**, *86*, 2241−2244.
(174) Mori-Sánchez, P.; Wu, Q.; Yang, W. Orbital-dependent correlation energy in density-functional theory based on a second-order perturbation approach: Success and failure. *J. Chem. Phys.* **2005**, *123*, No. 062204.
(175) Jiang, H.; Engel, E. Second-order Kohn-Sham perturbation theory: Correlation potential for atoms in a cavity. *J. Chem. Phys.* **2005**, *123*, 224102.
(176) Grabowski, I.; Teale, A. M.; Fabiano, E.; Śmiga, S.; Buksztel, A.; Della Sala, F. A density difference based analysis of orbital-dependent exchange-correlation functionals. *Mol. Phys.* **2014**, *112*, 700−710.
(177) Mezei, P. D.; Csonka, G. I.; Kállay, M. Electron Density Errors and Density-Driven Exchange-Correlation Energy Errors in Approximate Density Functional Calculations. *J. Chem. Theory Comput.* **2017**, *13*, 4753−4764 PMID: 28892613.
(178) Śmiga, S.; Buksztel, A.; Grabowski, I. Chapter 7 - Density-Dependent Exchange-Correlation Potentials Derived From highly Accurate Ab initio Calculations. In *Proceedings of MEST 2012: Electronic structure methods with applications to experimental chemistry*; Hoggan, P., Ed.; Adv. Quantum Chem.; *Academic Press*, 2014; Vol. *68*; pp. 125−151.
(179) Śmiga, S.; Della Sala, F.; Buksztel, A.; Grabowski, I.; Fabiano, E. Accurate Kohn-Sham ionization potentials from scaled-opposite-spin second-order optimized effective potential methods. *J. Comput. Chem.* **2016**, *37*, 2081−2090.
(180) Kamiya, M.; Hirata, S. Higher-order equation-of-motion coupled-cluster methods for ionization processes. *J. Chem. Phys.* **2006**, 125.
(181) Shavitt, I.; Bartlett, R. J. *Many-body methods in chemistry and physics: MBPT and coupled-cluster theory*; Cambridge university press, 2009.
(182) Goerigk, L.; Hansen, A.; Bauer, C.; Ehrlich, S.; Najibi, A.; Grimme, S. A look at the density functional theory zoo with the advanced GMTKN55 database for general main group thermochemistry, kinetics and noncovalent interactions. *Phys. Chem. Chem. Phys.* **2017**, *19*, 32184−32215.
(183) Curtiss, L. A.; Raghavachari, K.; Redfern, P. C.; Pople, J. A. Assessment of Gaussian-2 and density functional theories for the computation of enthalpies of formation. *J. Chem. Phys.* **1997**, *106*, 1063−1079.
(184) Curtiss, L. A.; Raghavachari, K.; Trucks, G. W.; Pople, J. A. Gaussian-2 theory for molecular energies of first- and second-row compounds. *J. Chem. Phys.* **1991**, *94*, 7221−7230.
(185) Goerigk, L.; Grimme, S. A General Database for Main Group Thermochemistry, Kinetics, and Noncovalent Interactions Assessment of Common and Reparameterized (meta-)GGA Density Functionals. *J. Chem. Theory Comput.* **2010**, *6*, 107−126 PMID: 26614324.
(186) Parthiban, S.; Martin, J. M. L. Assessment of W1 and W2 theories for the computation of electron affinities, ionization potentials, heats of formation, and proton affinities. *J. Chem. Phys.* **2001**, *114*, 6014−6029.
(187) Zhao, Y.; Truhlar, D. G. Density Functional for Spectroscopy: No Long-Range Self-Interaction Error, Good Performance for Rydberg and Charge-Transfer States, and Better Performance on Average than B3LYP for Ground States. *J. Phys. Chem. A* **2006**, *110*, 13126−13130.
(188) Zhao, Y.; Truhlar, D. G. Benchmark Databases for Nonbonded Interactions and Their Use To Test Density Functional Theory. *J. Chem. Theory Comput.* **2005**, *1*, 415−432.
(189) Zhao, Y.; Truhlar, D. G. Design of Density Functionals That Are Broadly Accurate for Thermochemistry, Thermochemical Kinetics, and Nonbonded Interactions. *J. Phys. Chem. A* **2005**, *109*, 5656−5667.
(190) Jurečka, P.; Šponer, J.; Černý, J.; Hobza, P. Benchmark database of accurate (MP2 and CCSD(T) complete basis set limit) interaction energies of small model complexes, DNA base pairs, and amino acid pairs. *Phys. Chem. Chem. Phys.* **2006**, *8*, 1985−1993.
(191) Marshall, M. S.; Burns, L. A.; Sherrill, C. D. Basis set convergence of the coupled-cluster correction, Î′MP2CCSD(T): Best practices for benchmarking non-covalent interactions and the attendant revision of the S22, NBC10, HBC6, and HSG databases. *J. Chem. Phys.* **2011**, *135*, 194102.
(192) Yihan, S.; et al. Advances in molecular quantum chemistry contained in the Q-Chem 4 program package. *Mol. Phys.* **2015**, *113*, 184−215.
(193) Valiev, M.; et al. NWChem: A comprehensive and scalable open-source solution for large scale molecular simulations. *Comput. Phys. Commun.* **2010**, *181*, 1477−1489.
(194) Fritsche, L. Generalized Kohn-Sham theory for electronic excitations in realistic systems. *Phys. Rev. B* **1986**, *33*, 3976−3989.
(195) Seidl, A.; Görling, A.; Vogl, P.; Majewski, J. A.; Levy, M. Generalized Kohn-Sham schemes and the band-gap problem. *Phys. Rev. B* **1996**, *53*, 3764.
(196) Fabiano, E.; Della Sala, F. Localized exchange-correlation potential from second-order self-energy for accurate Kohn-Sham energy gap. *J. Chem. Phys.* **2007**, *126*, 214102.
(197) Śmiga, S.; Siecińska, S.; Fabiano, E. Methods to generate reference total and Pauli kinetic potentials. *Phys. Rev. B* **2020**, *101*, 165144.
(198) Śmiga, S.; Constantin, L. A. Modified Interaction-Strength Interpolation Method as an Important Step toward Self-Consistent Calculations. *J. Chem. Theory Comput.* **2020**, 4983 PMID: 32559078.
(199) Görling, A. New KS method for molecules based on an exchange charge density generating the exact local KS exchange potential. *Phys. Rev. Lett.* **1999**, *83*, 5459−5462.
(200) Ivanov, S.; Hirata, S.; Bartlett, R. J. Exact exchange treatment for molecules in finite-basis-set Kohn-Sham theory. *Phys. Rev. Lett.* **1999**, *83*, 5455−5458.
(201) Jankowski, K.; Nowakowski, K.; Grabowski, I.; Wasilewski, J. Coverage of dynamic correlation effects by density functional theory functionals: Density-based analysis for neon. *J. Chem. Phys.* **2009**, *130*, 164102.
(202) Jankowski, K.; Nowakowski, K.; Grabowski, I.; Wasilewski, J. Ab initio dynamic correlation effects in density functional theories: a density based study for argon. *Theor. Chem. Acc.* **2010**, *125*, 433−444.
(203) Talman, J. D.; Shadwick, W. F. Optimized effective atomic central potential. *Phys. Rev. A* **1976**, *14*, 36−40.
(204) Witkowski, M.; Śmiga, S.; Grabowski, I. Chapter Sixteen - Density-Based Analysis of Spin-Resolved MP2 Method. In *Novel Electronic Structure Theory: General Innovations and Strongly Correlated Systems*; Hoggan, P. E., Ed.; Advances in Quantum Chemistry; Academic Press, 2018; Vol. *76*; pp. 279−293.
(205) Handy, N. C.; Schaefer, H. F., III On the evaluation of analytic energy derivatives for correlated wave functions. *J. Chem. Phys.* **1984**, *81*, 5031−5033.
(206) Bartlett, R. J. Analytical evaluation of gradients in coupled-cluster and many-body perturbation theory. In *Geometrical Derivatives of Energy Surfaces and Molecular Properties*; Jørgensen, P., Simons, J., Eds.; Reidel, Dordecht: The Netherlands, 1986; pp. 35−61.
(207) Salter, E. A.; Trucks, G. W.; Bartlett, R. J. Analytic energy derivatives in many-body methods. I. First derivatives. *J. Chem. Phys.* **1989**, *90*, 1752−1766.
(208) Jørgensen, P.; Helgaker, T. Møller−Plesset energy derivatives. *J. Chem. Phys.* **1988**, *89*, 1560−1570.
(209) Koch, H.; Jensen, H. J. A.; Jørgensen, P.; Helgaker, T.; Scuseria, G. E.; Schaefer, H. F., III; et al. *J. Chem. Phys.* **1990**, *92*, 4924−4940.
(210) Hald, K.; Halkier, A.; Jørgensen, P.; Coriani, S.; Hättig, C.; Helgaker, T. A Lagrangian, integral-density direct formulation and implementation of the analytic CCSD and CCSD(T) gradients. *J. Chem. Phys.* **2003**, *118*, 2985−2998.
(211) Peverati, R.; Head-Gordon, M. Orbital optimized double-hybrid density functionals. *J. Chem. Phys.* **2013**, *139*, No. 024110.

https://dx.doi.org/10.1021/acs.jctc.0c00823
J. Chem. Theory Comput. 2020, 16, 7413−7430

(212) Sancho-Garca, J. C.; Pérez-Jiménez, A. J.; Savarese, M.; Brémond, E.; Adamo, C. Importance of Orbital Optimization for Double-Hybrid Density Functionals: Application of the OO-PBE-QIDH Model for Closed- and Open-Shell Systems. *J.Phys. Chem. A* **2016**, *120*, 1756−1762 PMID: 26901447.
(213) Gu, Y.; Xu, X. Extended Koopmans' theorem in the adiabatic connection formalism: Applied to doubly hybrid density functionals. *J. Chem. Phys.* **2020**, *153*, No. 044109.
(214) Stanton, J. F.; et al., *ACES II*; Quantum Theory Project: Gainesville, Florida, 2007.
(215) Śmiga, S.; Grabowski, I. Spin-Component-Scaled ΔMP2 Parametrization: Toward a Simple and Reliable Method for Ionization Energies. *J. Chem. Theory Comput.* **2018**, *14*, 4780−4790 30040889.
(216) Śmiga, S.; Siecińska, S.; Grabowski, I. From simple molecules to nanotubes. Reliable predictions of ionization potentials from the ΔMP2-SCS methods. *New J. Phys.* **2020**, *22*, No. 083084.
(217) Cohen, A. J.; Mori-Sánchez, P.; Yang, W. Second-Order Perturbation Theory with Fractional Charges and Fractional Spins. *J. Chem. Theory Comput.* **2009**, *5*, 786−792 26609584.
(218) Parrish, R. M.; et al. Psi4 1.1: An Open-Source Electronic Structure Program Emphasizing Automation, Advanced Libraries, and Interoperability. *J. Chem. Theory Comput.* **2017**, *13*, 3185−3197 28489372.

https://dx.doi.org/10.1021/acs.jctc.0c00823
J. Chem. Theory Comput. 2020, 16, 7413−7430